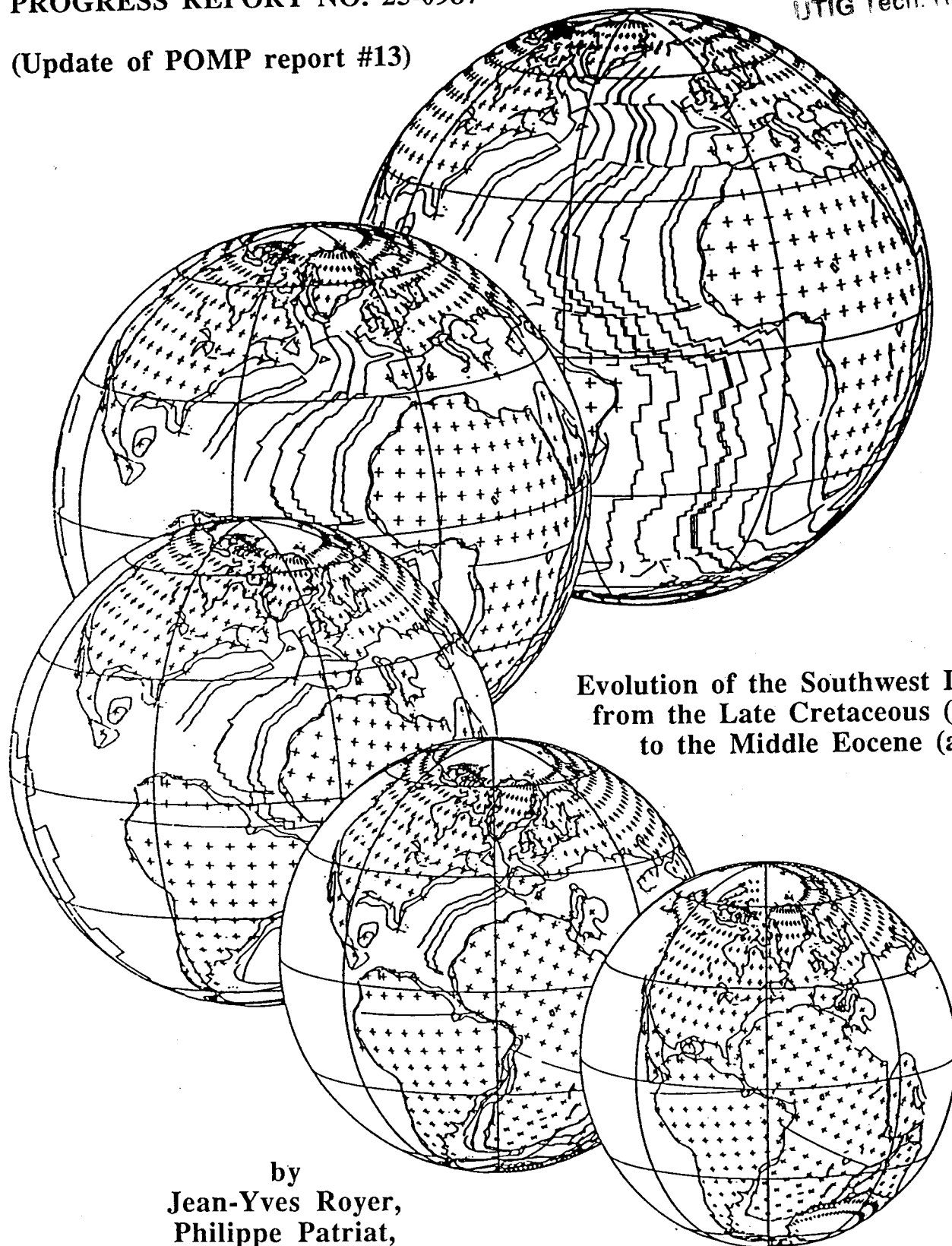


**PALEOCEANOGRAPHIC MAPPING PROJECT
PROGRESS REPORT NO. 25-0987**

Library
UTIG Tech. Report # 76

(Update of POMP report #13)



**Evolution of the Southwest Indian Ridge
from the Late Cretaceous (anomaly 34)
to the Middle Eocene (anomaly 20).**

by
**Jean-Yves Royer,
Philippe Patriat,
Hugh W. Bergh
& Christopher R. Scotese**

**Evolution of the Southwest Indian Ridge from the Late Cretaceous
(anomaly 34) to the Middle Eocene (anomaly 20).**

*Jean-Yves Royer **

*Philippe Patriat ***

*Hugh W. Bergh ****

*Christopher R. Scotese * †*

* Institute for Geophysics
University of Texas at Austin
8701 Mopac Boulevard
Austin Texas 78759

** Laboratoire de Géophysique Marine et CNRS UA 279
Institut de Physique du Globe de Paris
4 place Jussieu
75230 Paris cedex 05 France

*** Bernard Price Institute of Geophysical Research
University of Witwatersrand
1 Jan Smuts Avenue
Johannesburg 2001 South Africa

† now at: Shell Development Company
Bellaire Research Center
P.O. Box 481
Houston Texas 77001

Tectonophysics

August 1987

Abstract

The determination of the motion of Antarctica relative to Africa is particularly important when considering the breakup of Gondwana. Two models have been proposed that describe the pattern of seafloor spreading between Africa and Antarctica during the Late Cretaceous (starting at chron 34, 84 Ma) through to the Middle Eocene (chron 20, 46 Ma). In the first model, the motion of Antarctica relative to Africa can be simply described by a rotation about a single pole of rotation. In the second model, which we favor, the relative motion of Antarctica and Africa is more complex, and a major change in spreading direction between chron 32 (74 Ma) and chron 24 (56 Ma) times is required.

In this paper we present 10 plate tectonic reconstructions of the Southwest Indian Ridge that were produced using a new compilation of magnetic, bathymetric, and satellite altimetry data, in combination with interactive computer graphics. These reconstructions illustrate that spreading directions started to change at chron 32 time (74 Ma). Between chrons 31 and 28 (69 to 64 Ma), spreading was very slow (<1 cm/yr) and the direction of spreading changed from NE-SW to a more N-S direction. Between chrons 26 and 24 (61 to 56 Ma) the direction of spreading shifted back to a NE-SW orientation. These changes in spreading direction suggest that the present-day fracture zones in the area of the Prince Edward fracture zone are younger features (Eocene) than their lengths might imply. Our results also provide important constraints concerning the Mesozoic reconstructions of the Indian Ocean and the motion of South America relative to Antarctica prior to the Eocene.

Introduction

The history of relative motion between Africa and Antarctica is the key to understanding the dispersal of the fragments of Gondwana, after their initial breakup in the Late Jurassic. The occurrence of a Paleocene fossil ridge in the Mascarene Basin (Schlich, 1982), separating Madagascar from the Seychelles-Saya de Malha Bank, makes it difficult to resolve the motion of Africa relative to India prior to chron 29 time (66 Ma). Similarly, the complex development of the Scotia Sea and the interaction of the South Sandwich trench with the American-Antarctic Ridge (Barker et al., 1984) do not permit direct determination of the relative motion between South

America and Antarctica prior to chron 21 time (50 Ma). Therefore, models of the evolution of the Indian Ocean depend heavily on an understanding of the relative motions of Africa with respect to Antarctica, South America with respect to Africa (Ladd, 1974; Cande et al., 1986), and India with respect to Antarctica (Patriat, 1983). Though magnetic anomalies indicate that seafloor spreading between Africa and Antarctica has been taking place since the Late Jurassic, the relative motion of these two continents is not well constrained. This paper describes the seafloor spreading history along the Southwest Indian Ridge during the Late Cretaceous and Early Tertiary (chron 34 - chron 20).

The early history of seafloor spreading between Africa and Antarctica can be reconstructed using the identifications of Mesozoic magnetic anomalies (M22 - M0) in the Mozambique Channel (Ségoufin, 1978; Simpson et al., 1979) and their counterparts to the south, in the vicinity of Dronning Maud Land (Bergh, 1977). Exactly how these sets of magnetic anomalies must be matched, however, is still controversial (Norton and Sclater, 1979; Ségoufin and Patriat, 1981; Martin and Hartnady, 1986). Disagreements arise from the fact that there is no data from the Cretaceous Quiet Zone (118 - 84 Ma) and that various reconstructions have been proposed for the configuration of the Southwest Indian Ridge at chron 34 time (84 Ma).

In contrast, the Eocene to Recent development of the Southwest Indian Ridge is better understood, and has been investigated in detail between 46°E and 70°E (Fig. 1) (Patriat, 1979, 1983; Tapscott et al., 1980; Sclater et al., 1981). From chron 20 time (46 Ma) to the present, the Southwest Indian Ridge has been spreading very slowly (<1 cm/yr) in a N-S direction. Although plate reconstructions for this time interval are based on data from only the eastern part of the Southwest Indian Ridge, the rotation parameters are well constrained by symmetric sets of magnetic anomalies, and the results are in good agreement with rotations calculated by solving the plate circuit Africa-India-Antarctica (Patriat, 1983; Patriat and Ségoufin, this volume).

Because of the remoteness of Antarctica and the paucity of oceanographic surveys at high southerly latitudes, the magnetic anomaly data that describes the period of seafloor spreading between the Late Cretaceous (chron 34, 84 Ma) and the Middle Eocene (Chron 20, 46 Ma) come primarily from the area north of the Southwest Indian Ridge. Late Cretaceous and Early Tertiary magnetic anomalies have been described from the Agulhas Basin, Mozambique Basin, and in the southwest portion of the Madagascar Basin (LaBrecque and Hayes, 1979; Bergh and Norton, 1976; Patriat, 1979). Magnetic anomalies in these areas are often difficult to identify due to slow spreading rates, the occurrence of numerous volcanic edifices, and the extremely rugged topography resulting from the complex system of deep, en échelon fracture zones (Fig. 1).

Because of the poor constraints provided by the magnetic data, some of the first reconstructions of Africa and Antarctica were based on the assumption that the continuous trends of well-defined fracture zones, such as the Prince Edward fracture zone, were "flow-lines" that described the relative motion between Africa and Antarctica since the Late Cretaceous. This assumption led to the conclusion that the motion between Africa and Antarctica during the last 80 million years could be modeled by a single rotation about a stationary Euler pole (Norton and Sclater, 1979; Fisher and Sclater, 1983). This simple assumption was challenged, however, by new identifications of anomalies 33 (80 Ma) and 34 (84 Ma) in the vicinity of the Prince Edward fracture zone (Fig. 1) by Patriat et al. (1985). Their identifications required that a significant change in spreading direction must have taken place between chron 32 (74 Ma) and chron 24 (56 Ma) times. This change in spreading direction, also illustrated by Larson et al. (1985), suggests that large offset fracture zones, such as the Prince Edward fracture zone, are not as continuous as they appear, and consequently, they can not be used to derive rotation parameters for long periods of time.

In this paper we present a new compilation of magnetic, bathymetric and satellite altimetry data (Seasat) that documents the change in spreading direction along the Southwest Indian Ridge during the Late Cretaceous and Early Tertiary. These data, in conjunction with the Evans and Sutherland interactive computer graphics system, has been used to produce plate tectonic reconstructions of Africa and Antarctica for chrons 34 (84 Ma), 33 (80 Ma), 32 (74 Ma), 31 (69 Ma), 29 (66 Ma), 28 (64 Ma), 26 (61 Ma), 24 (56 Ma), 21 (50 Ma), and 20 (46 Ma). The area of investigation is centered on the Prince Edward Fracture Zone and extends from 5°E to 65°E, and from 20°S to 65°S (Fig. 1).

Data compilation

Bathymetry and magnetic anomalies

Our compilation is based mainly on bathymetric and magnetic data published in the scientific literature during the last decade. Our bathymetric interpretations are based on the work of Driscoll et al. (in press), Fisher and Sclater (1983) and Sclater et al. (1981), as well as the GEBCO oceanographic survey (LaBrecque and Rabinowitz, 1981; Hayes and Vogel, 1981; Fisher et al., 1982). The magnetic compilation is based on information from the National Geophysical Data Center, and unpublished magnetic data collected by South African research vessels, south of the

Southwest Indian Ridge and in the Agulhas Basin. These new profiles are shown on Plate 1 and some of the profiles from the African-Antarctic Basin are interpreted on Figure 2. All the magnetic anomaly data have been reinterpreted using the magnetic reversal time scale of Kent and Gradstein (1986). Table 1 presents the reversal boundaries that have been picked on magnetic profiles. These boundaries are the same as those used by Patriat (1983), Patriat et al. (1985) and Barker and Lawver (submitted). The magnetic anomalies east of 46°E or those related to the Central and the Southeast Indian Ridges, are from Patriat (1983). The magnetic anomaly data in these areas have been published by Schlich (1975, 1982).

Satellite altimetry data

Satellite altimetry data have proved exceptionally useful in remote and uncharted oceanic areas. The excellent correlation between the small wavelength features of the geoid and seafloor topography has been widely used to map topographic features such as fracture zones (e.g. Sandwell and Schubert, 1982) or uncharted seamounts (e.g. Lazarewick and Schwank, 1982). Recently, Driscoll et al. (in press) have tested the usefulness of this approach by comparing deflection of the vertical with bathymetry in a particularly rugged and well charted area near the Southwest Indian Ridge between 20°E and 50°E. They showed that the lineations seen in the geoid gradient closely follow the fracture zone trends although their actual locations remain difficult to determine from the geoid data alone. This is especially the case where the fracture zones are closely spaced, as in the area between the du Toit and the Prince Edward Fracture Zones. Using a similar analysis described by Gahagan et al. (this volume), we have correlated the highs and lows of the deflection of the vertical in order to determine the azimuth of the fracture zones where only sparse bathymetric data were available.

The Southwest Indian Ridge between 5°E and 65°E

Bathymetry

a) Fracture zones

The topography of the southwestern Indian Ocean floor is characterized by a series of deep and well delineated fracture zones. As outlined by the GEBCO chart (Fisher et al., 1982), the

main fracture zones are expressed by narrow and deep troughs, with depths sometimes greater than 6000m, bordered by elevated rims, in some places shallower than 2000m. A comprehensive survey of the westernmost du Toit, Bain and Prince Edward Fracture Zones has been made by Driscoll et al. (in press), and similar work for the Discovery, Indomed and Galliéni Fracture Zones, has been published by Fisher and Sclater (1983). Sclater et al. (1981) described the easternmost Atlantis II and Melville Fracture Zones (Fig. 1).

All these fracture zones extend over great distances, have nearly continuous trends and are subparallel. The structural grain, emphasized by deep troughs, strikes 15° to 20° NE near Prince Edward Fracture Zone. This regular pattern and the alignment of these fracture zones with older structures such as the Mozambique plateau, has led to the interpretation that these fracture zones represent flow-lines that describe the motions of Africa relative to Antarctica since the Late Cretaceous (Norton and Sclater, 1979; Fisher and Sclater, 1983).

There are relatively little bathymetric data south of 55°S, as illustrated by the artificially smooth and uniform contours on the most up-to-date bathymetric map of this area (GEBCO sheet 5•13). This lack of detail contrasts with the complex meandering of the bathymetric contours north of the Southwest Indian Ridge (see GEBCO sheet 5•9). South of the Southwest Indian Ridge it is not possible to locate the counterpart of the Mozambique Fracture Zone or to follow the southern extension of the du Toit Fracture Zone. Satellite altimetry data (Seasat), however, provides additional data as far south as 65°S. The satellite-gravity map of Haxby (1985), in addition to highlighting the linearity of the fracture zones north of the South Indian Ridge, revealed a major N-NE, S-SW trending structure in the Enderby Basin. The southern extension of this feature appears to join the Astrid Ridge and corresponds to the Astrid Fracture Zone described by Bergh (1987). Although the Astrid Fracture Zone appears to be aligned with the Prince Edward Fracture Zone, a clearly defined westward shift of the Astrid Fracture Zone at about 56°S indicates that its northerly continuation is the Bain Fracture Zone (Fig. 3). The observed westward shift of fracture zone trends at 56°S is the best evidence for the proposed change in spreading direction during the Late Cretaceous.

At present, the largest offset of the Southwest Indian Ridge axis lies between the Prince Edward and du Toit Fracture Zones. The active parts of these fracture zones intersect the ridge axis at about 45°S, 35°E and 53°S, 27°E, respectively. Over the relatively short distance between these two fracture zones (< 200 km), the ridge axis is offset by more than 7° (~ 800 km). Rough topography makes it difficult to identify additional ridge segments between the Prince Edward and Du Toit Fracture Zones.

It is interesting to note that the location of the large offset in the Southwest Indian Ridge axis has shifted through time. The minor offset of anomaly 34 in the Mozambique Basin (Bergh and Norton, 1976) indicates that the offset of the Late Cretaceous ridge axis, north of the Prince Edward Fracture Zone was relatively small (< 250 km). During the Late Cretaceous, the major offset in the ridge axis was between the Mozambique Ridge and the magnetic bight in the Agulhas Basin (Fig. 3). The magnetic anomaly data require that either a ridge jump or a change in spreading direction took place sometime between the Late Cretaceous (84 Ma) and the Eocene (chron 20; 46 Ma).

b) Aseismic ridges

Several aseismic ridges occur in the western Indian Ocean that are symmetrically disposed on either side of the Southwest Indian Ridge. The westernmost pair of aseismic ridges are the Agulhas Plateau and the Maud Rise (Fig. 3). These features lie north and south, respectively, of chron 34 and therefore are probably Middle Cretaceous in age. Further to the east, stand two other features: the Mozambique Ridge and the Astrid Ridge (Fig. 3). Although it has not been clearly established whether these ridges are continental or oceanic in origin, their position with respect to anomaly 34 indicates that they are older than Late Cretaceous. We believe that during the Middle Cretaceous the Agulhas Plateau was joined together with the Maud Rise, and the Mozambique Ridge was aligned with the Astrid Ridge. This realignment requires that there was motion oblique to present-day fracture zone trends, sometime after the Late Cretaceous.

Further to the east are the Madagascar Ridge and the Del Caño and Conrad Rises, which lie south of the ridge axis. The northern portion of the Madagascar Ridge is composed of an anomalous type of crust, that may be partly continental in origin, while the southern part of the ridge is considered to be thickened oceanic crust (Goslin et al., 1981; Sinha et al., 1981; Recq and Goslin, 1981). To the west of the southern Madagascar Ridge is ocean floor of early Late Cretaceous age (anomaly 34; Bergh and Norton, 1976); to the east of the southern Madagascar Ridge is ocean floor of that is Paleocene in age (anomaly 29; Patriat, 1979). The oldest magnetic anomaly immediately to the south of the Madagascar Ridge is Eocene in age (anomaly 22; Fisher and Sclater, 1983).

The Del Caño Rise consists of volcanic edifices and seamounts that trend east-west and extend between the Prince Edward and Marion Islands, on the west, and the Crozet Archipelago and Crozet Bank, on the east. The deep seismic structure of the Del Caño Rise resembles that of

typical oceanic crust and because of its similarity to the southern portion of the Madagascar Ridge, it has been proposed that both features were formed at the same time along the axis of the Southwest Indian Ridge (Goslin et al., 1981). The orientation of the Del Caño Rise relative to the ridge axis suggests either that spreading has been very asymmetric or that the Del Caño Rise has been growing in a westerly direction; however, there are no published magnetic anomalies between the Del Caño Rise and the ridge axis that might lend support to either of these hypotheses. The entire region north of the Del Caño Rise is also anomalously elevated (Anderson et al., 1973) and corresponds to a positive anomaly in the geoid (Roufousse et al., 1981).

Unlike the Del Caño Rise, the age of the ocean floor surrounding the Crozet Bank is well known. The Crozet Bank is bounded by anomaly 32 to the southwest and by anomaly 31 to the northeast (Schlich, 1975; Fig. 3). Both of these magnetic anomalies were generated along the axis of the Southeast Indian Ridge. Just to the northwest of the Crozet Bank lies anomaly 29 (Fig. 3) that was produced by spreading along the Southwest Indian Ridge (Patriat, 1979).

South of the Del Caño Rise and Crozet Bank lies the broad, W-NW trending Conrad Rise that consists, in part, of the Ob, Lena and Marion Dufresne seamount chain (Fig. 1). During the Late Cretaceous the Lena and Marion Dufresne seamounts formed the southern limit of the Crozet Basin (Schlich, 1975, 1982) which was related to spreading along the Southeast Indian Ridge. To the north and east of the Ob seamount, Patriat et al. (1985) have recently identified magnetic anomalies 33 and 34, produced by spreading along the Southwest Indian Ridge. Gravity studies indicate that the Ob, Lena and Marion Dufresne seamounts are locally isostatically compensated (Goslin, 1979; Diament and Goslin, 1986).

Kinematic considerations led Goslin and Patriat (1984) to suggest that the Marion Dufresne, Lena and Ob seamounts, as well as the southern portion of the Madagascar Ridge and Del Caño Rise were formed at ridge axes rather than by intraplate volcanism. They proposed that the southern Madagascar Ridge and Del Caño Rise were produced along the Southwest Indian Ridge during a period of slow spreading in the Early Eocene (chrons 24 - 23; 55 Ma). The Ob, Lena and Marion Dufresne seamounts are older and may have been generated during a major reorganization of the plate boundaries during the Cretaceous Quiet Zone (Diament and Goslin, 1986). The time of the uplift of the Crozet Bank remains uncertain. Geoid studies (Cazenave et al., 1980) suggests that the bank may be the result of recent intraplate volcanism, whereas the pattern of magnetic anomalies and evidence of local isostatic compensation suggest a much older age (Goslin, 1981).

Magnetic anomalies

In the African-Antarctic Basin, seafloor spreading since the Late Cretaceous is now well documented by numerous magnetic profiles (Plate 1; LaBrecque and Hayes, 1979; Bergh, 1986; LaBrecque and Cande, 1986). The magnetic anomaly sequences are complete on both side of the ridge from anomaly 34 to present and show a slow decrease in spreading rates from 4.7 cm/yr at chron 34 time (84 Ma) to 0.8 cm/yr at present. As illustrated in Figure 2, a period of very slow spreading occurred between chrons 31 and 28. During the same time interval, sea floor spreading stopped in both the Cape Basin, south of the Falkland-Agulhas fracture zone, and in the Mascarene Basin, between Madagascar and the Seychelles-Saya de Malha Bank (Schlich, 1982). LaBrecque and Hayes (1979) and Bergh and Barrett (1980) have mapped the magnetic bight on the African plate formed by anomalies 33 and 34, southwest of the Agulhas Plateau. Bergh and Barrett (1980) also identified the corresponding bight on the Antarctic plate, north of Maud Rise. The location of the magnetic bight indicates that the triple junction between the African, Antarctic and South American plates at chron 33 and 34 times separated the Agulhas Plateau and Maud Rise. Further to the east, on the Antarctic plate, Norton and Sclater (1979) identified anomalies 34 through 31. The easternmost identification of anomaly 34 lies west of the Astrid Ridge, just 2° north of the Mesozoic anomalies identified by Bergh (1977).

The first good identification of Late Cretaceous and Early Cenozoic magnetic anomalies along the Southwest Indian Ridge were made in the Mozambique Basin, east of the Prince Edward Fracture Zone (Bergh and Norton, 1976). They suggested that there were two abrupt changes in spreading rates: one during the Middle/Late Eocene (between anomalies 21 and 15) and second during the Late Oligocene/Early Miocene (between anomalies 8 and 5). Recent reinterpretations of these data by Ségoufin (1981) and Fisher and Sclater (1983) have favored a more continuous spreading rate between anomalies 24 and 13, followed by a significant decrease in rates after anomaly 13 (1.4 to 0.8 cm/yr). The revised spreading rates has permitted the identification of magnetic anomalies 21 through 13 along profiles south of the ridge axis, and are consistent with spreading rates in the African-Antarctic Basin during the same time interval (Fig. 2; LaBrecque and Hayes, 1979; Bergh, 1986).

The other well defined anomalies in the Mozambique Basin are of Late Cretaceous to Paleocene age (anomalies 34 to 28). Ségoufin (1981) identified another set anomalies 34 to 32, east of the southern part of the Mozambique Ridge. This anomaly sequence has been considered to be offset from anomalies 34 to 31 further to the east by the northern extension of the Prince Edward Fracture Zone (Fig. 3). Spreading rates for these anomalies are equivalent to those reported for the African-Antarctic Basin during the same time interval (4.0 cm/yr from anomaly 34

to 33 and 1.5 cm/yr from anomaly 33 to 28). Between anomalies 28 and 24 in the Mozambique Basin, no clear interpretation can be made. The distance between these anomalies implies a high spreading rate (3.6 cm/yr) which is not observed either in the African-Antarctic Basin or in the Madagascar Basin.

South of the ridge axis and east of the Prince Edward Fracture Zone, anomalies 33 and 34 are clearly identified (Bergh and Barrett, 1980; Ségoufin and Patriat, 1981). Patriat et al. (1985) confirmed these identifications with new profiles collected by the R/V Marion Dufresne between the "southern extension" of the Prince Edward Fracture Zone and the Conrad Rise. In addition, they mapped two other 34-32 sequences that stair-step to the north and east. These identifications play a key role in constraining reconstructions for chron 33 and 34 times. One of their profiles runs from anomaly 34 to the ridge axis, and indicates a period of very slow spreading between chron 32 and 24 times. This contrasts with the accelerated spreading rates to the north of the ridge axis during the same time interval. This asymmetry in spreading rates suggests that a ridge jump, to the south, occurred east of the Prince Edward Fracture Zone between chron 28 and 24 times.

East of the Indomed Fracture Zone (46°E), Patriat (1979, 1983) identified several sets of anomalies 13 through 29 on either side of the Southwest Indian Ridge and calculated a spreading rate of 1.4 cm/yr for that time interval. It is interesting to note that the age of the oldest magnetic anomalies decreases to the east: anomaly 29 is not observed east of the Galliéni Fracture Zone (53°E), anomaly 24 is not observed east of the Atlantis II Fracture Zone (57°E), and anomaly 20 is not observed east of the Melville Fracture Zone (61°E). This pattern is the result of the rapid eastward migration of the Indian Ocean triple junction, combined with slow spreading along the Southwest Indian Ridge. Sclater et al. (1981) recognized that a similar pattern is observed for anomalies 19 and younger between the Melville Fracture Zone to the Rodriguez Triple Junction (25°S, 70°E).

Isochrons from the northern flank of the Southwest Indian Ridge intersect the isochrons created along the Central Indian Ridge in the Madagascar Basin. Their intersections form acute, chevron-shaped bights. Isochrons from the southern flank of the Southwest Indian Ridge intersect the isochrons generated along the Southeast Indian Ridge in the Crozet Basin, where they form obtuse bights. The apexes of these bights represent the past location of the triple junction between the African, Antarctic and Indian plates (Patriat and Courtillot, 1984) and provide important constraints for plate tectonic reconstructions.

In the African-Antarctic Basin the variable trends of anomalies 32 through 24 (Plate 1) are consistent with the suggestion that spreading directions changed dramatically during this interval.

However, east of the Prince Edward fracture zone, magnetic anomaly data does not provide any direct evidence for a change of spreading direction. The only indication that a major plate reorganization took place is the asymmetry of spreading rates, north and south of the ridge axis, between chron 28 and chron 24 times.

Reconstructions

Method

The poles and angles of the finite rotations (Table 2) were calculated with the method described by Patriat (1983). The parameters of rotation were determined by matching magnetic picks from both sides of the Southwest Indian Ridge and minimizing the area of misfit (sum of triple scalar products; p. 526, McKenzie and Sclater, 1971). Data from the fracture zones were not used in these calculations because of the difficulty in precisely locating the traces of conjugate transform faults. We believe that the reconstructions presented in Figures 6a to 6j are well constrained due to the geometrical constraints provided by large offsets in the ridge axis, the relative abundance of magnetic data, the variable orientation of magnetic lineations, and the length of plate boundary under study (2000 to 3500 km).

An attempt has been made to avoid drastic, and probably spurious, changes in spreading rates and directions. In this regard, the evolution of spreading rates and directions through time (Fig. 5, Table 4) has been used as an independent check of the plate reconstruction model. This is especially true for those intervals when magnetic picks are sparse or when symmetric magnetic picks are lacking (e.g. anomaly 31). Also, as mentioned earlier, the reconstruction of the triple junctions at either end of the Southwest Indian Ridge provides important additional constraints.

Relative motions of Antarctica and Africa from the Late Cretaceous (anomaly 34) to the Middle Eocene (anomaly 20).

The set of finite rotations presented in Table 2 and illustrated Figure 4a, describes the relative motion of Antarctica and Africa for 10 stages during the Late Cretaceous and Early Tertiary (chron 34, 84 Ma through chron 20, 46 Ma). The chron 34 and 33 finite poles are within 1 degree of the poles determined by Patriat et al. (1985). The finite poles for chron 29 through chron 20 are also

quite well constrained by the magnetic data. On the other hand, the chron 32 and chron 31 poles are less well constrained and two alternate models are possible. In the first model, the direction of spreading remains nearly constant between chrons 33 and 32. The finite pole at chron 32 time is 4.3°S , 41.3°W (angle= 13.51°), and the finite pole at chron 31 time is 5.6°N , 48.0°W (angle= 11.74°) (Fig. 4a). This model requires that a drastic change in spreading direction occurred between chrons 31 and 29. In the Agulhas Basin, for instance, the spreading direction would had to have changed by 47° and the spreading rate would had to have increased from 2 cm/yr to 5 cm/yr. We favor an alternate model which suggests that spreading rates and directions changed more continuously between chrons 33 and 29, as observed on Plate 1 and Figure 2. The stage poles (Table 3) that we derive follow a hook-shaped curve that doubles-back on itself between chron 31-29 (Fig. 4b). A similar cusp is observed at the same time on the stage pole wandering path that describes the opening of the South Atlantic Ocean (Cande et al., 1986).

Table 4 and Figure 5 display the rates and directions of spreading calculated along two flow-lines, one located in the Agulhas Basin and the other, east of the Prince Edward Fracture Zone. The resulting curve confirms the change in relative plate motion proposed by Patriat et al. (1985). The change in spreading directions is nearly continuous and can be divided in three episodes (Fig. 5). During the first episode (chron 34 to chron 29; 84 to 66 Ma) spreading directions progressively shift from SSW-NNE to SSE-NNW, and spreading rates fall by a factor of 3. During this episode an important step in spreading direction occurs at chron 33. The next change in spreading direction, interestingly, does not appear to be synchronous along the ridge. Changes in spreading direction first take place in the Agulhas Basin (chron 31), and then propagate eastward towards the Prince Edward Fracture Zone (chron 29). These changes in spreading direction are contemporaneous with the extinction of the Mid-Atlantic Ridge in the Cape Basin, south of the Agulhas-Falkland Fracture Zone (Du Plessis, 1977; Barker, 1979; LaBrecque and Hayes, 1979). From chron 29 to chron 24 times (66 to 56 Ma), the direction of spreading shifts backward to SSW-NNE. The second phase ends with a reorganization of the plate boundary that begins at about chron 26 (61 Ma). The third and final episode of spreading begins at chron 24 (56 Ma), and by chron 20 (46 Ma) the direction and rate spreading are similar to present-day plate motions. East of Prince Edward Fracture Zone, our computed direction of spreading is 15° NE. This is the same as the spreading direction estimated by Bergh and Norton (1976), and similar to the direction (17° NE) reported by Sclater et al. (1981). It is interesting to note that these directions of spreading are nearly the same as the spreading directions between chrons 34 and 33.

Reconstructions of the Southwest Indian Ridge configuration

In this section we present plate tectonic reconstructions of the Southwest Indian Ridge at chron 34, 33, 32, 31, 29, 28, 26, 24, 21, and 20 (Fig. 6a to 6j). These reconstructions are based on our compilation of available magnetic, bathymetric, and satellite altimetry data (Plate 1, Fig. 1 and 3). For each reconstruction we have drawn isochrons that illustrate the past configuration of the Southwest Indian Ridge. The location of transform faults has been deduced from bathymetric and satellite altimetry data, and the trend of the transform faults are small circles about the stage poles that describe the relative plate motions during the intervening time intervals. The ridge segments are drawn on the basis of observed and rotated magnetic picks, or in a manner consistent with the previous ridge configuration.

Chrons 34 and 33 (Fig. 6a and 6b) have both been drawn using the 34-33 stage pole to determine fracture zone trends. One of the main features of the chron 34 reconstruction is the huge offset of the ridge axis between the Mozambique Basin and the Agulhas Basin. This offset, which we call the Agulhas-Mozambique Fracture Zone, was created as a result of differential spreading in the Agulhas and Mozambique Basins. Sea floor spreading began in the Mozambique and Enderby Basin during the Late Jurassic as a result of the separation of Africa and Antarctica. Rifting, however, did not begin in the Agulhas Basin until the separation of South America (Falkland Plateau) and Africa during Early Cretaceous. In the African-Antarctic Basin, there is no evidence of Mesozoic anomalies related to Africa-Antarctica motions; furthermore, chron 34 lies at the same distance from the African and Antarctic coastlines (approx. 10°).

The direction of spreading before chron 34 time was probably parallel to the trend of the Mozambique Ridge, which we consider to be the northern counterpart of the Astrid Fracture Zone. At chron 34 time, the Conrad Rise was adjacent to the Madagascar Ridge, though it is likely that these two features had separated shortly before chron 34 time. Patriat and Goslin (1984) argue that a ridge jumped north, from the Enderby Basin to the Conrad Rise, sometime near the end of the Cretaceous Quiet Zone (approx. 90 Ma). This ridge jump may have been synchronous with the initiation of spreading between Madagascar and the Seychelles-India block.

The change in spreading direction between chron 33 and 32 times required that the Agulhas-Mozambique Fracture Zone, south of the Mozambique Plateau, break up into a staircase succession of small ridge and transform fault segments (Fig. 6c). Our representation of the number and location of the ridge segments is arbitrary; however the trend of the transform faults matches the trend of the fracture zone shift between the Astrid and Bain Fracture Zones (Fig. 3). It

is important to note that the configuration of the ridge axis at chron 32 time severely constrains subsequent configurations of the Southwest Indian Ridge.

The configuration of the Southwest Indian Ridge at chron 31, 29, and 28 times is very similar (Fig. 6d to 6f). Due to the rapid change in spreading directions and as a result of the very slow rates, spreading was highly oblique during this period. Ridge segments increased in length as the direction of motion shifted NW-SE. The Crozet Bank may have been created at the ridge axis between chron 32 and 31 times, however, because there is no counterpart on the Indian plate, it is more likely to be the result of younger intraplate volcanism.

At chron 26 time (Fig. 6g), the configuration of the ridge in the African-Antarctic Basin began to change. However, as in the case of the earlier reconstructions, there are only few identified anomalies between 32°E and 46°E. Chron 24 time marks the end of the phase of oblique spreading. By that time, spreading directions and the orientation of the Southwest Indian Ridge became similar to the present configuration (Fig. 6h). Between chron 26 and 24 times several ridge jumps occurred in the Mozambique Basin. East of 38°E a ridge segment jumped to the south; between the Madagascar Ridge and Del Caño Rise, another two ridge segments jumped to the north. The large offset in the ridge along the Galliéni Fracture Zone was created by a ridge jump at this time. The dashed lines in Figures 6h to 6j indicate the extinct ridge axes. As a result of the change in plate motion, the ridge segments west of Prince Edward Fracture Zone shortened, while the offsets between the ridge segments grew longer (Fig. 6h to 6j). By chron 20 time, the growing fracture zone offsets had coalesced to form the basis of the modern Bain-Prince Edward Fracture Zone system.

One of the special aspects of the Southwest Indian Ridge is the fact that since the Late Cretaceous, it has been bounded by triple junctions each involving three mid-oceanic ridges. At chron 34, 33, and 32 times, we assume that the Indian-African-Antarctic triple junction had a R-F-F configuration and that its location remained fixed with respect to the African plate. This configuration resulted in the lengthening of the Southeast Indian Ridge. The rapid eastward migration of the Indian-African-Antarctic triple junction started after chron 32 time, when the spreading rates slowed down between Africa and Antarctica, while increasing rapidly between Africa and India and between India and Antarctica. Since that time the Indian triple junction has had alternatively a R-R-F or R-R-R configuration (Patriat and Courtillot, 1984). The rate of lengthening of the Africa - Antarctica plate boundary was very high between chron 31 and chron 28 times (~ 140 km/Ma; Table 5) with spreading rates along the Central and Southeast Indian ridges 8 times greater than spreading rates along the Southwest Indian Ridge.

When the directions and rates of spreading began to change along the Southwest Indian Ridge (chron 26) and along the Central and Southeast Indian Ridges (chron 24), the eastward migration of the Indian-African-Antarctic triple junction began to slow down. The large fracture zones south of the Madagascar Basin, such as the Atlantis II and Melville Fracture Zones, originated during this time interval (chron 24 and chron 20 respectively). The Indian-African-Antarctic triple junction has been migrating eastward at a nearly constant rate (~30 km/Ma) since the Middle Eocene. The V-shaped domain, apparent in both the bathymetric and magnetic data, is due to the fact that the eastward migration rate of the triple junction has always been greater than the spreading rate along the Southwest Indian Ridge.

At the western end of the Southwest Indian Ridge, the Africa-South America-Antarctic triple junction has migrated westward during the same time interval. Between chron 34 and 33 times, and possibly until chron 31 time, the triple junction was an R-F-F type (LaBrecque and Hayes, 1979; Bergh and Barrett, 1980). After the westward jump of the ridge that occurred at about chron 31 time, the triple junction migrated south of Meteor Rise. At that time, the Mid-Atlantic Ridge and the Southwest Indian Ridge were probably linked by a long fracture zone running south of Meteor Rise.

Implications and discussion

One aspect of this work concerns the behavior and evolution of the important fracture zones that characterize the Southwest Indian Ridge in the vicinity of the Prince Edward Fracture Zone. Initially, they were considered to be stable features, whose location and orientation had not substantially changed since chron 34 time (Norton and Sclater, 1979; Fisher and Sclater, 1983; Martin and Hartnady, 1986). However, Patriat et al. (1985) have shown that these fracture zones are not stable and that the ridge-fracture zone geometry has changed with time.

Several lines of evidence have lead us to conclude that the fracture zones along the central portion of the Southwest Indian Ridge are not stable features. A change in plate motion, and a consequent change in fracture zone geometry, is required if one compares the reconstruction of the Southwest Indian Ridge at chron 33 or 34 time with its present configuration. At chron 33 and 34 times, the long fracture zone that separated magnetic anomalies in the Mozambique and Agulhas Basins (Agulhas-Mozambique Fracture Zone) ran along the eastern edge of the Mozambique Ridge (Fig. 6a and 6b). This configuration was inherited from the Early Cretaceous, during which time

the eastern edge of the Mozambique Ridge was aligned with the Astrid Fracture Zone. At present, however, the long offset fracture zone (Prince Edward Fracture Zone) is no longer aligned with the Mozambique Ridge. This suggests that there has been either a shift in the location of the fracture zone or reorganization of fracture zone geometry.

We believe that the reconstruction at chron 34 and 33 times are particularly well constrained because the large offset along the Agulhas-Mozambique Fracture Zone, combined with the relative abundance of magnetic picks, results in a unique fit of Africa and Antarctica. Patriat et al. (1985) also noted that the character of the magnetic signature (amplitudes and symmetry) is similar for conjugate magnetic anomalies from the Mozambique and Enderby Basins. Furthermore, chrons 28 and 29 are consistent and well constrained, and provide the required intermediate steps between chrons 31 and 26. The good agreement of our rotation parameters with those obtained by closing the plate circuit Africa-India-Antarctica (Patriat, 1983; Patriat and Ségoufin, this issue) provides an independent verification of our results between chrons 29 and 20 (Fig. 6e to 6j).

Though a variety of magnetic evidence is available, there is little bathymetric evidence for the proposed change in plate motion. When the chrons 20 or 21 are superimposed on the new bathymetric summary of Driscoll et al. (in press), it becomes apparent that the well-mapped fracture zones, trending NNE-SSW, lie between these isochrons and therefore are younger features. Between the eastern edge of the Mozambique Ridge and chrons 20 and 21, bathymetric data are scarce and no particular structural trends emerge. To the north, the only bathymetric evidence for the change in motion is a topographic high bordered by a deep fracture that shifts from a NNE-SSW direction (48°S , 31°E) to a N-S direction (45°S , 32°E). In the vicinity of Antarctica, detailed bathymetry is lacking, but satellite altimetry data provides clear evidence for the change in plate motion (Fig. 3). Considering the drastic change in spreading direction between chron 29 and 24 times, the slow spreading rates, and the time span involved (~ 30 Ma), it is not surprising that a stable system of fracture zones did not develop. Well-defined fracture zones did not become reestablished until the modern system of plate motion became established at chron 21 time.

An indirect argument in favor of the proposed change in plate motion is that other plate reorganizations occurred in the southern oceans between chron 31 and 24 times. In the South Atlantic Ocean, spreading rates dropped abruptly at about chron 31 time and direction of spreading changed slightly (Cande et al., 1986). Sometime between chrons 31 and 28, the Mid-Atlantic Ridge in the Cape Basin stopped spreading; spreading resumed west of Meteor Rise at chron 26-25 time (Barker, 1979; LaBrecque and Hayes, 1979). In the Indian Ocean, seafloor spreading ceased in the Mascarene Basin shortly after chron 28 time (Schlich, 1982). The fast northward

drift of India also started at chron 31 time. Evidence for a rapid and nearly simultaneous increase in spreading rates at chron 31 time is found in the Crozet, Madagascar and Central Indian Basins, as well as in the Mascarene and Wharton Basin (McKenzie and Sclater, 1971; Sclater and Fisher, 1974; Schlich, 1975, 1982). At chron 22 time, spreading rates in these basins began to slow down. This phase of spreading ended in middle Eocene due to the collision of India and Asia and the resulting plate boundary reorganization.

In conclusion, it must be emphasized that this rapid change in motion may have modified and reshaped the topography as well as the fracture zone pattern. The Agulhas-Mozambique and Astrid Fracture Zones have been spared because they stand outside and now bound the restructured area. Therefore, except for these two old fracture zones, the present fracture zones (i.e. Prince Edward Fracture Zone) only reflect the direction of spreading during the last 45 million years, and are much younger than their lengths might imply.

Conclusion

By matching magnetic anomalies symmetrically disposed along the Southwest Indian Ridge, we have derived a set of rotation parameters that confirm the important change in relative motion between Africa and Antarctica during the Late Cretaceous and Early Tertiary, first pointed out by Patriat et al. (1985) and Larson et al. (1985). This change in relative plate motion began at chron 32 time (74 Ma), and during the latest Cretaceous (chron 31 to chron 28; 71 to 66 Ma), the direction of spreading shifted nearly 45° to the northwest. During the earliest Tertiary (chron 26 to chron 24; 61 to 56 Ma) the direction of motion shifted back to the original spreading direction. By the Early Eocene (chron 21 - chron 20; 50 to 46 Ma), the Southwest Indian Ridge had adopted its present-day configuration.

By accurately reconstructing the history of relative motion between Antarctica and Africa, we have provided new constraints concerning the breakup of Gondwana. Our reconstructions are a starting point for further work, in particular: the Mesozoic evolution of the Indian Ocean, the evolution of the plate boundary between South America and Antarctica, and the development of the Weddell Sea and Scotia Sea.

The complex evolution of the Southwest Indian Ridge, especially in the vicinity of the Prince Edward Fracture Zone, underscores the fact that fracture zone trends cannot always be taken at

face value and should be used with great care for determining relative plate motions. The last direction of motion can easily overprint and erase previous transform fault trends. Furthermore, in areas of slow spreading rates and rough topography, complex changes in past plate motions may be easily overlooked.

Acknowledgements: The authors wish to thank Mavis Driscoll and John LaBrecque for their helpful comments and suggestions. This work was supported, in part, by a Shell Distinguished Professorship to John G. Sclater, and by the sponsors of the Paleooceanographic Mapping Project (POMP), University of Texas at Austin. The senior author also received support while at the Institute for Geophysics, University of Texas from the French Foreign Office ("bourse Lavoisier"). This is UTIG contribution n° 726.

References

- Anderson R. N., McKenzie D. P. & Sclater J. G., 1973: Gravity, bathymetry and convection in the earth. Geophys. J. R. astr. Soc., 34: 137-147.
- Barker P. F., 1979: The history of ridge-crest offset at the Falkland-Agulhas fracture zone from a small-circle geophysical profile. Geophys. J. Roy. astr. Soc., 59: 131-145.
- Barker P. F. and Lawver L. A., (submitted): The Cenozoic evolution of the South American-Antarctic Ridge. Geophys. J. Roy. astr. Soc.
- Barker P. F., Barker P. L. & King E. C., 1984: An early Miocene ridge crest-trench collision on the South Scotia Ridge near 36°W. Tectonophysics, 102: 317-332.
- Bergh H. W., 1977: Mesozoic seafloor off Dronning Maud Land, Antarctica. Nature, 269: 686-687.
- Bergh H. W., 1986: Seafloor spreading symmetry between Africa and Antarctica. S. Afr. J. Ant. Res., 16: 9-12.
- Bergh H. W., 1987: Underlying fracture zone nature of Astrid Ridge off Antarctica's Queen Maud Land. J. Geophys. Res., 92: 475-484.
- Bergh H. W. & Barrett D. M., 1980: Agulhas Basin magnetic bight. Nature, 287: 591-595
- Bergh H. W. & Norton I. O., 1976: Prince Edward fracture zone and the evolution of the Mozambique Basin. J. Geophys. Res., 81: 5221-5239.
- Cande S. C., LaBrecque J. L., Haxby W. F., Mello S. & Rowley D. C., 1986: A high resolution seafloor spreading history of the South Atlantic (abstract). Presented at the Geodynamics Symposium, Texas A & M, April 23-25, 1986.
- Cazenave A., Lago B., Dominh K. & Lambeck K., 1980: On the response of the ocean lithosphere to seamounts loads from GEOS3 satellite radar altimeter observations. Geophys. J. R. astr. Soc., 63: 233-252.

- Diament M. & Goslin J., 1986: Emplacement of the Marion Dufresne, Lena and Ob seamounts (South Indian Ocean) from a study of isostasy. Tectonophysics, 121: 253-262.
- Driscoll M. L., Fisher R. L. & Parsons B., (in press): Fracture zone trends and structure of the Southwest Indian Ridge: an investigation using Seasat altimetry and surface-ship bathymetry. Geophys. J. R. astr. Soc.
- Du Plessis, 1977: Seafloor spreading south of the Agulhas fracture zone. Nature, 270: 719-721.
- Fisher R. L. & Sclater J. G., 1983: Tectonic evolution of the Southwest Indian Ridge since the Mid-Cretaceous: plate motions and stability of the pole of Antarctica/Africa for at least 80 Ma. Geophys. J. R. astr. Soc., 73: 553-576.
- Fisher R. L., Jantsch M. Z. & Comer R. L., 1982: General Bathymetric Chart of the Ocean: sheet 5•9. Canadian Hydrographic Service, Ottawa, Canada.
- Gahagan L. M., Royer J.-Y., Scotese C. R., Sandwell D. T., Winn K., Ross M. I., Newman J. S., Müller D., Mayes C. L., Lawver L. A., Huebeck C. E. & Coffin M., (this issue): Tectonic fabric map of the ocean basins from satellite altimetry data. Tectonophysics.
- Goslin J., 1979: Résultats de gravimétrie sur les monts sous-marins du Marion Dufresne, de la Léna et de l'Ob (Océan Indien austral). C. R. Ac. Sci., 288 (B): 241-244.
- Goslin J., 1981: Etude géophysique des reliefs aismiques de l'océan Indien occidental et austral. Thèse de Doctorat d'Etat, Université Louis Pasteur, Strasbourg, 267 pp.
- Goslin J. & Patriat P., 1984: Absolute and relative plate motions and hypotheses on the origin of five aseismic ridges in the Indian Ocean. Tectonophysics, 101: 221-244.
- Goslin J., Recq M. & Schlich R., 1981: Structure profonde du plateau de Madagascar: relations avec le plateau de Crozet. Tectonophysics, 76: 75-97.
- Haxby W. F., 1985: Gravity field of World's Oceans (color map). Lamont Doherty Geological Observatory.

- Hayes D. E. & Vogel M., 1981: General Bathymetric Chart of the Ocean: sheet 5•13. Canadian Hydrographic Service, Ottawa, Canada.
- Kent D. V. & Gradstein F. M., 1986: A Jurassic to recent chronology. In: P. R. Vogt and B. E. Tucholke (eds), The geology of North America: The Western Atlantic region, volume M: 45-50, Geol. Soc. Am.
- LaBrecque J. L. & Hayes D. E., 1979: Seafloor spreading history of the Agulhas Basin. Earth Planet. Sci. Lett., 45: 411-428.
- LaBrecque J. L. & Rabinowitz P. D., 1981: General Bathymetric Chart of the Ocean: sheet 5•16. Canadian Hydrographic Service, Ottawa, Canada.
- LaBrecque J. L. & Cande S. C., 1986: Total intensity magnetic anomaly profiles. In Ocean Margin Drilling Regional Atlas 13, South Atlantic Ocean and Adjacent Continental Margin, J. L. LaBrecque ed., Marine Science International, Woods Hole.
- Ladd J. W., 1974: South Atlantic seafloor spreading and Caribbean tectonics. Ph. D. Thesis, Columbia University, New-York, 251 pp.
- Larson R. L., Pitman W. C., Golovchenko X., Cande S. C., Dewey J. F., Haxby W. F. & LaBrecque J. L., 1985: The Bedrock Geology of the World, W. H. Freeman Co., New-York NY.
- Lazarewicz A. R. & Schwank D. C., 1982: Detection of uncharted seamounts using satellite altimetry. Geophys. Res. Lett., 9: 385-388.
- Martin A. K. & Hartnady C. J. H., 1986: Plate tectonic development of the Southwest Indian Ocean: a revised reconstruction of East Antarctica and Africa. J. Geophys. Res., 91: 4767-4786.
- McKenzie D. P. & Sclater J. G., 1971: The evolution of the Indian Ocean since the Late Cretaceous. Geophys. J. R. astr. Soc., 25: 437-528.
- Norton I. O. & Sclater J. G., 1979: A model for the evolution of the Indian Ocean and the breakup of Gondwanaland. J. Geophys. Res., 84, 6803-6830.

- Patriat P., 1979: L'océan Indien occidental: la dorsale ouest-indienne. Mém. Mus. Nat. Hist. Nat., 43: 49-52.
- Patriat P., 1983: Evolution du système de dorsales de l'Océan Indien. Thèse de Doctorat d'Etat, Université Pierre et Marie Curie, Paris.
- Patriat P. & Courtillot V., 1984: On the stability of triple junctions and its relation to episodicity in spreading. Tectonics, 3: 317-332.
- Patriat P. & Ségoufin J., (this issue): Reconstructions of the Central and Western Indian Ocean. Tectonophysics.
- Patriat P., Ségoufin J., Goslin J. & Beuzart P., 1985: Relative positions of Africa and Antarctica in the Upper Cretaceous: evidence for a non-stationary behaviour of fracture zones. Earth Planet. Sci. Lett., 75: 204-214.
- Recq. M. & Goslin J., 1981: Etude de l'équilibre isostatique dans le sud-ouest de l'océan Indien à l'aide de résultats de réfraction sismique. Mar. Geol., 41: M1-M10.
- Sandwell D. T. & Schubert G., 1982: Geoid height-age relation from Seasat altimeter profiles across the Mendocino fracture zone. J. Geophys. Res., 87: 3949-3958.
- Schlich R., 1975: Structure et age de l'océan Indien occidental. Mém. hors série Soc. Geol. France, 6: 103 pp.
- Schlich R., 1982: The Indian Ocean: aseismic ridges, spreading centers and basins. In: A. E. Nairn and F. G. Stheli (eds), *The Ocean Basins and Margins: the Indian Ocean*, Plenum Press, New-York, 6: 51-147.
- Sclater J. G. & Fisher R. L., 1974: Evolution of the east-central Indian Ocean, with emphasis on the tectonic setting of the Ninetyeast Ridge. Geol. Soc. Am. Bull., 85: 683-702.
- Sclater J. G., Fisher R. L., Patriat P., Tapscott C. & Parsons B., 1981: Eocene to recent development of the Southwest Indian Ridge, a consequence of the evolution of the Indian Ocean triple junction. Geophys. J. R. astr. Soc., 64: 587-604.

- Ségoufin J., 1978: Anomalies magnétiques mésozoïques dans le bassin de Mozambique. C. R. Ac. Sci., 287: 109-112.
- Ségoufin J., 1981: Morphologie et structure du canal de Mozambique. Thèse de Doctorat d'Etat, Université Louis Pasteur, Strasbourg, 236 pp.
- Ségoufin J. & Patriat P., 1981: Reconstructions de l'océan Indien occidental pour les époques des anomalies M21, M2 et 34. Paléoposition de Madagascar. Bull. Soc. Géol. France, XXIII: 693-707.
- Simpson E. S. W., Sclater J. G., Parsons B., Norton I. O. & Meinke L., 1979: Mesozoic magnetic lineations in the Mozambique Basin. Earth Planet. Sci. Lett., 43: 260-264.
- Sinha M. C., Loudon K. E. & Parsons B., 1981: The crustal structure of the Madagascar Ridge. Geophys. J. R. astr. Soc., 66: 351-377.
- Tapscott C., Patriat P., Fisher R. L., Sclater J. G., Hoskins H. & Parsons B., 1980: The Indian Ocean triple junction. J. Geophys. Res., 85: 4723-4739.

Table 1. Ages of the magnetic reversal boundaries picked on our magnetic profiles, after the reversal timescale from Kent and Gradstein (1986). Ages correspond to the oldest boundary of normal polarity event, except those referenced with a y (youngest extremity).

Anomaly #	Age [Ma]
20	46.17
21	50.34
24	56.14
26	60.75
28y	64.29
29	66.17
31y	68.52
32	73.55
33	80.17
34y	84.00

Table 2. Finite rotations describing the motion of Antarctica relative to Africa.

Anomaly #	Age [Ma]	Latitude [+°N]	Longitude [+°E]	Angle [°]	N	Ω
20	46.2	11.4	-43.7	7.81	8	0.020
21	50.3	10.3	-42.9	8.77	7	0.014
24	56.1	6.7	-40.6	9.97	7	0.035
26	60.8	3.8	-39.7	10.63	4	0.038
28	64.3	0.6	-39.2	11.32	5	0.017
29	66.2	-0.4	-39.4	11.59	5	0.045
31	68.5	1.1	-41.6	11.84	3	0.011
32	73.6	-1.8	-41.4	13.47	5	0.020
33	80.2	-4.7	-39.7	16.04	11	0.004
34	84.0	-2.0	-39.2	17.85	12	0.003

Angles are positive counterclockwise. N is the number of points from the rotated contour matched with N+1 to 2N points from the fixed contour (i.e. N triple scalar products). The misfit area is evaluated by the mean value (Ω) of the N triple scalar products. Ω is expressed in $R^3 \cdot \pi^2 / 180^2 \text{ km}^3$ with R for earth radius.

Table 3. Stage poles and angles of rotation computed from the finite rotations of Table 2.

Anomalies #	Time span [Ma]	African plate		Angle		Antarctic plate	
		Latitude [+°N]	Longitude [+°E]	[°]	[°/Ma]	Latitude [+°N]	Longitude [+°E]
20-0	46.2	11.4	-43.7	7.81	0.17	11.4	-43.7
21-20	4.1	1.9	-36.0	0.98	0.24	1.0	-37.3
24-21	5.8	-15.6	-23.5	1.39	0.24	-18.2	-27.6
26-24	4.7	-31.1	-23.8	0.86	0.18	-33.4	-31.0
28-26	3.5	-38.2	-27.3	0.93	0.27	-39.6	-36.5
29-28	1.9	-36.7	-43.5	0.34	0.18	-35.1	-51.7
31-29	2.3	25.8	-103.0	0.60	0.26	36.0	-99.7
32-31	5.1	-21.5	-37.5	1.75	0.34	-21.8	-42.4
33-32	6.6	-17.8	-28.8	2.71	0.41	-20.3	-32.9
34-33	3.8	20.7	-38.6	1.98	0.52	19.4	-31.4

Angles are positive counterclockwise.

Table 4. Directions (D) and full rates (v) of spreading in the Agulhas and the Mozambique Basins. Δ is the distance in degrees between the stage pole of motion and the point of measurement.

Anomalies #	Time span [Ma]	Aghulas Basin				Prince Edward F.Z.			
		Δ [°]	v [cm/yr]	D Afr. [-°W, +°E]	D Ant.	Δ [°]	v [cm/yr]	D Afr. [-°W, +°E]	D Ant.
20-0	46.2	81	1.9	-149N	31N	91	1.9	-165N	15N
21-20	4.1	69	2.5	-151N	35N	79	2.6	-167N	15N
24-21	5.8	48	2.0	-152N	35N	58	2.3	-173N	9N
26-24	4.7	37	1.2	-169N	20N	50	1.5	170N	-7N
28-26	3.5	35	1.7	178N	8N	49	2.2	160N	-16N
29-28	1.9	47	1.4	169N	0N	61	1.7	154N	-21N
31-29	2.3	131	2.2	175N	6N	144	1.7	170N	-6N
32-31	5.1	52	3.0	-171N	19N	65	3.5	172N	-4N
33-32	6.6	49	3.4	-161N	31N	60	4.0	180N	4N
34-33	3.8	85	5.8	-143N	52N	92	5.8	-155N	31N

Table 5. Rate of lengthening (R) of the eastern extremity of the Southwest Indian Ridge from the Early Paleocene (anomaly 32) to present-day. The length of the plate boundary (L) is estimated by adding the ridge and transform fault segments from the Indomed Fracture Zone.

Anomaly #	L [km]	Time span [Ma]	R [km/Ma]
32	0		
		-----5.1	60
31	308		
		-----2.3	145
29	641		
		-----1.9	140
28	908		
		-----3.5	98
26	1250		
		-----4.7	90
24	1671		
		-----5.8	73
21	2095		
		-----4.1	28
20	2209		
		-----46.2	31
present	3644		

Figure captions

Plate 1: Profiles of residual magnetic anomalies at right angles to tracks in the Southwest Indian Ocean. South African research vessels' tracks are represented by dashed lines and NGDC data by plain lines.

Figure 1: Tectonic elements of the Southwest Indian Ridge. Contours are coastlines, limits of the continental shelf and 2000 and 4000 meters isobaths. Dotted lines show the structural grain according to the bathymetric deeps. The present ridge axis (heavy line) is traced from bathymetry, Seasat data, axial magnetic anomalies and earthquake epicenters .

Figure 2: Interpretation of magnetic anomalies from some profiles in the African-Antarctic Basin. All profiles are projected onto direction N20°E. Extremities of profiles (A, B, C, D and E) are located on Plate 1.

Figure 3: Compilation of magnetic anomalies and Seasat lineations. Seasat data are taken from the ascending subsatellite tracks only: dotted lines join lineated maxima of the deviation of the vertical, and dashed lines, minima.

Figure 4: Wandering paths of a) finite and b) stage poles of rotation (see Tables 2 & 3 for coordinates). Stage poles are shown for the northern flank or African side of the Southwest Indian Ridge.

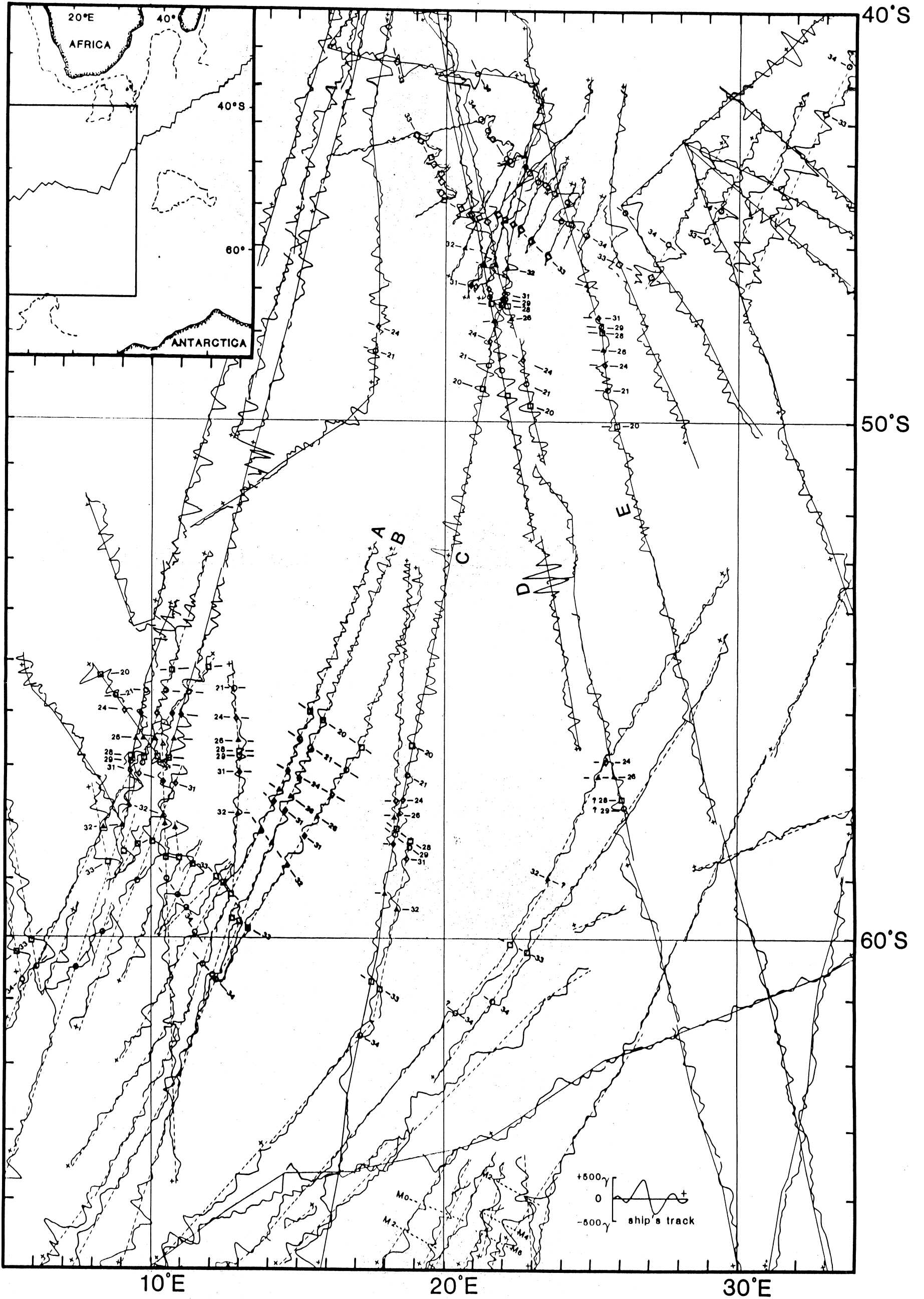
Figure 5: Evolution of the rates and directions of spreading of the Southwest Indian Ridge between the Late Cretaceous and the Middle Eocene. These parameters (Table 4) are computed for the Agulhas Basin (dashed line) and the Mozambique Basin (plain line); directions of spreading correspond to the northern flank of the ridge.

Figure 6a to 6j: Configurations of the Southwest Indian Ridge at 10 stages of its evolution between the Late Cretaceous and the Middle Eocene. Circles are magnetic picks from the African plate, triangles from the Antarctic plate and squares from the Indian plate. Contours are identical to those on Figure 1. Finite rotations at chron 34, 33, 32, 31 and 29 times between India and Antarctica, and from chron 28 to 20 times between India and Africa are from Patriat (1983).

Plate 1

Evolution of the Southwest Indian Ridge from the Late Cretaceous (anomaly 34) to the Middle Eocene (anomaly 20).

Royer J.-Y., Patriat P., Bergh H.W., Scotese C. R., Tectonophysics.



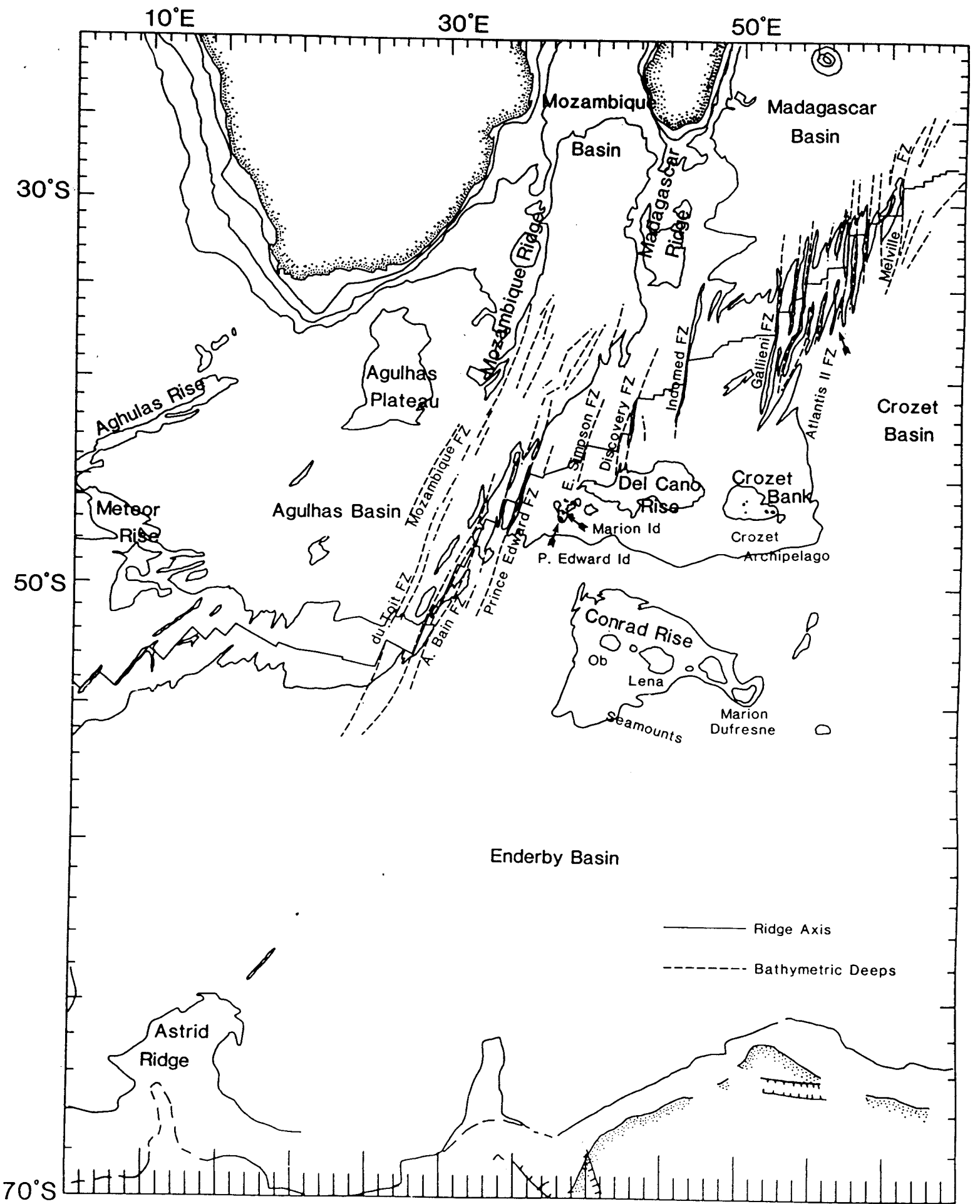


Figure 1

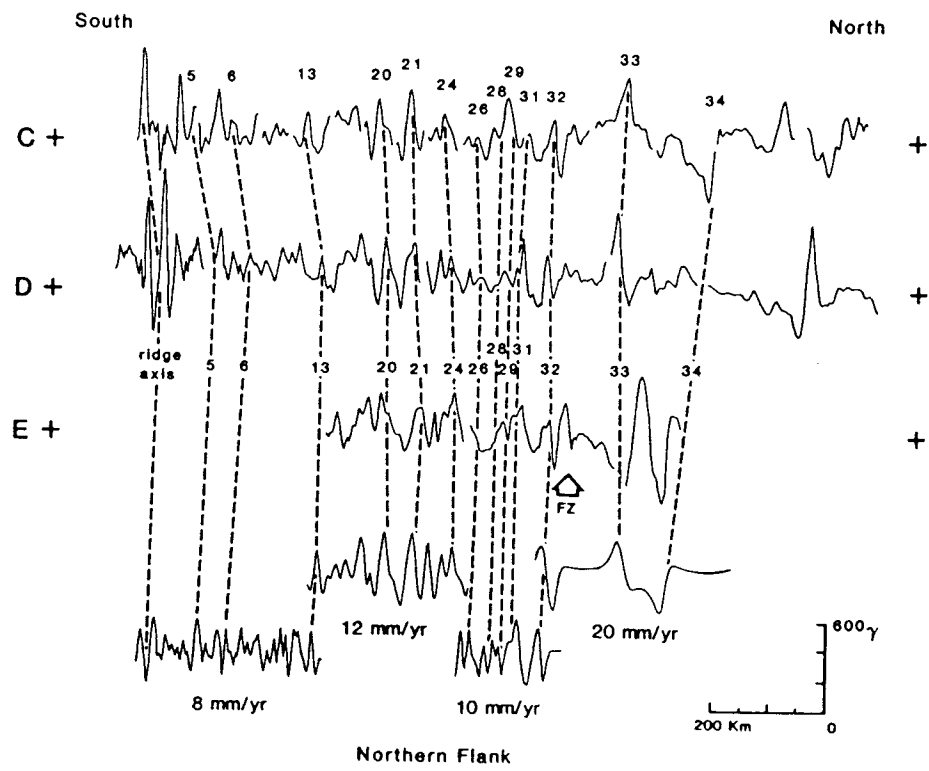
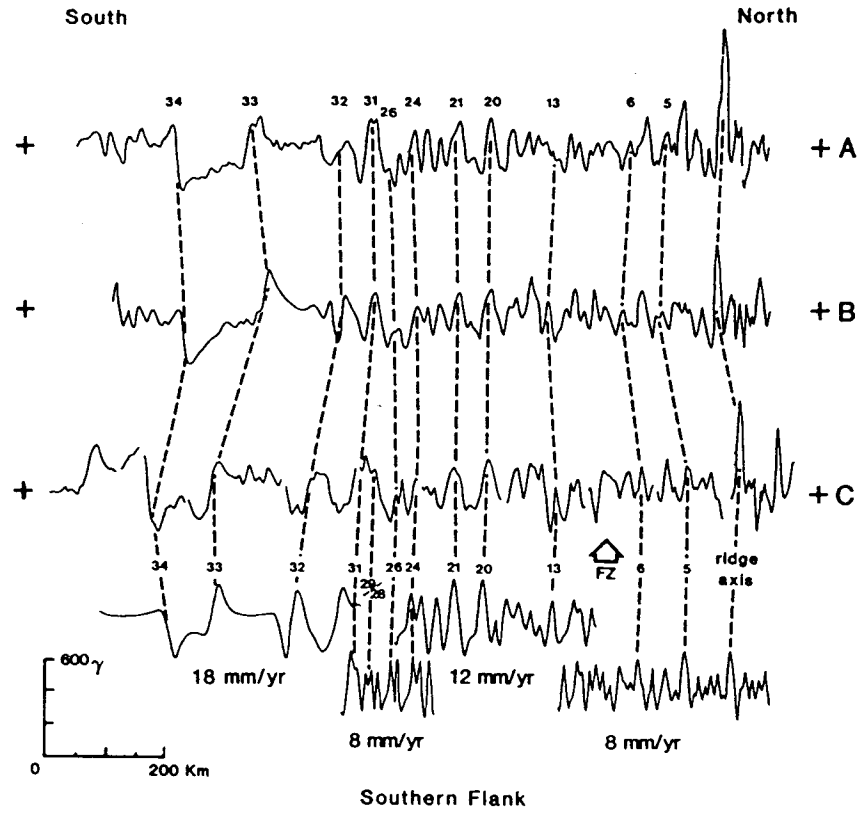


Figure 2

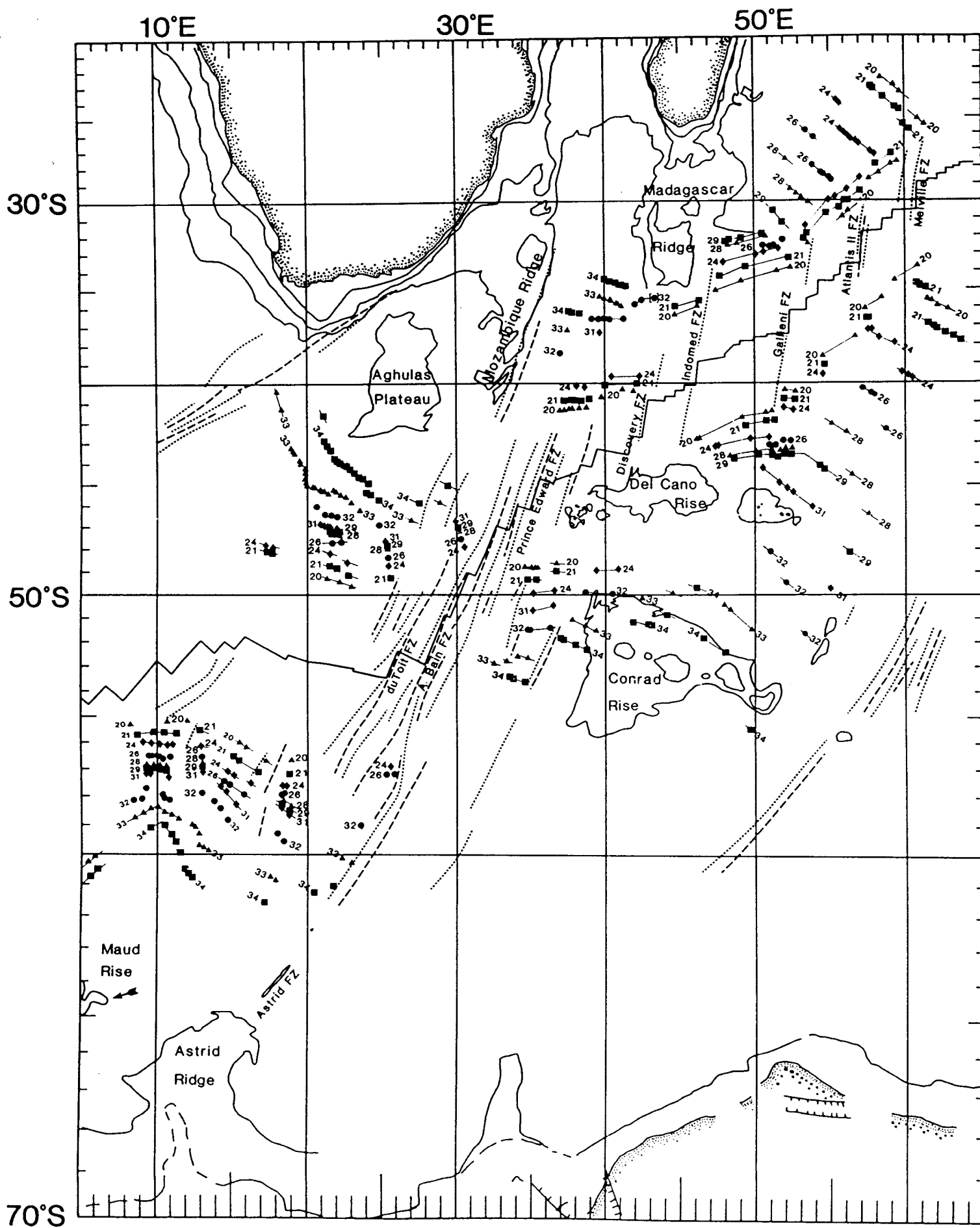


Figure 3

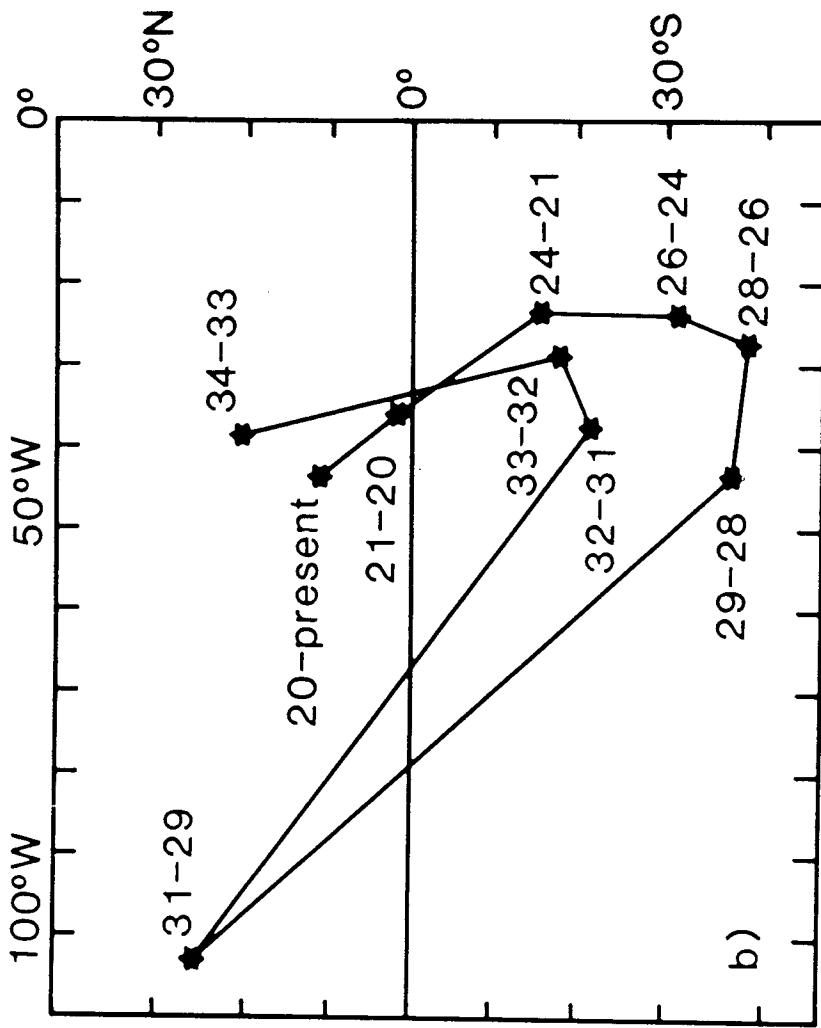
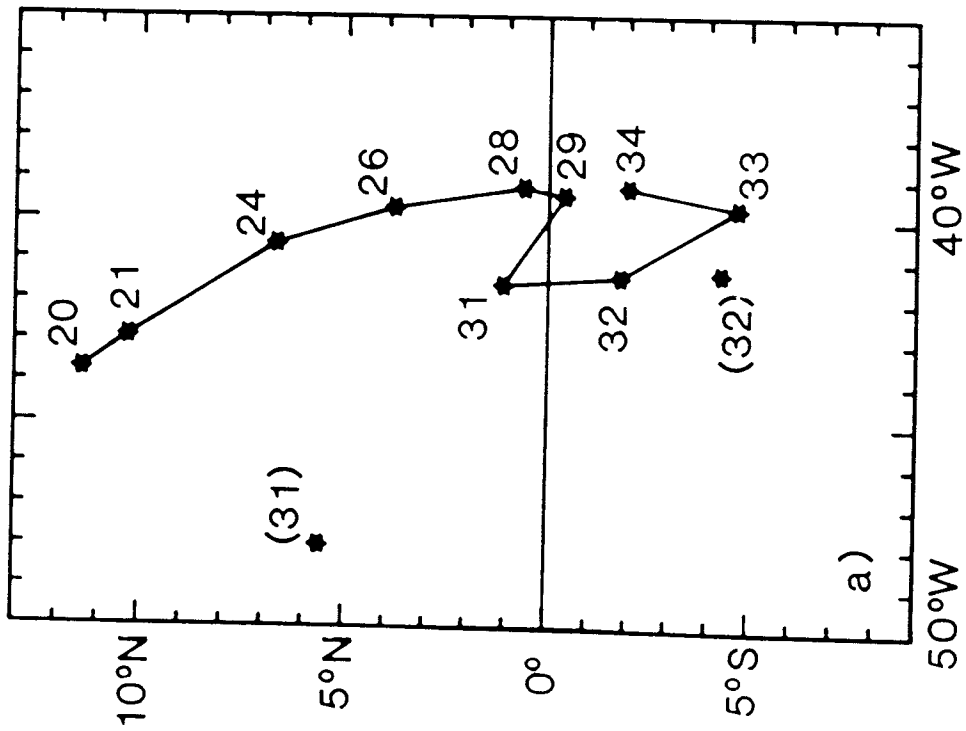


Figure 4

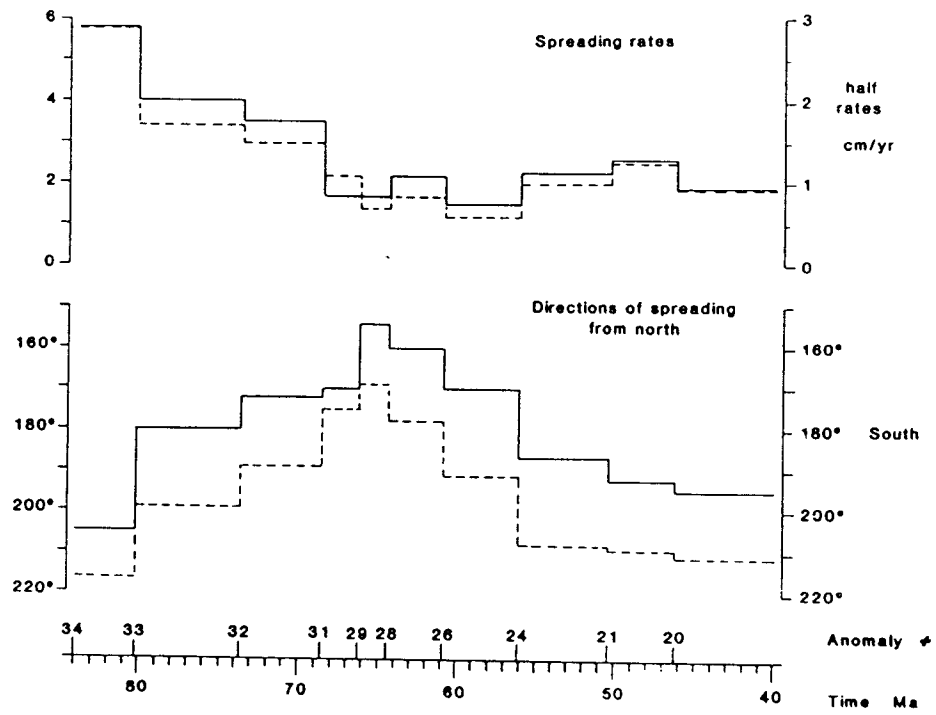


Figure 5

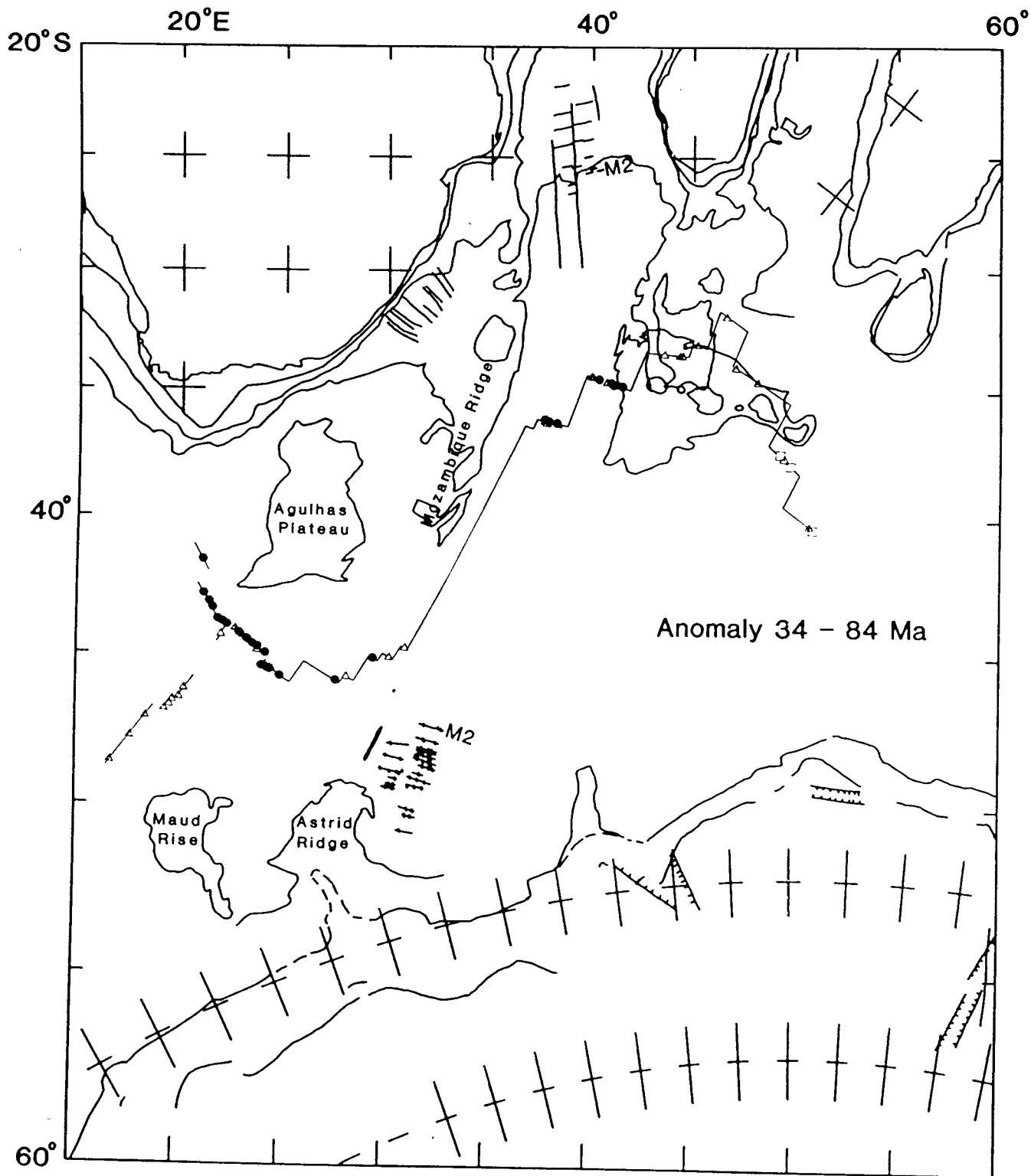


Figure 6a

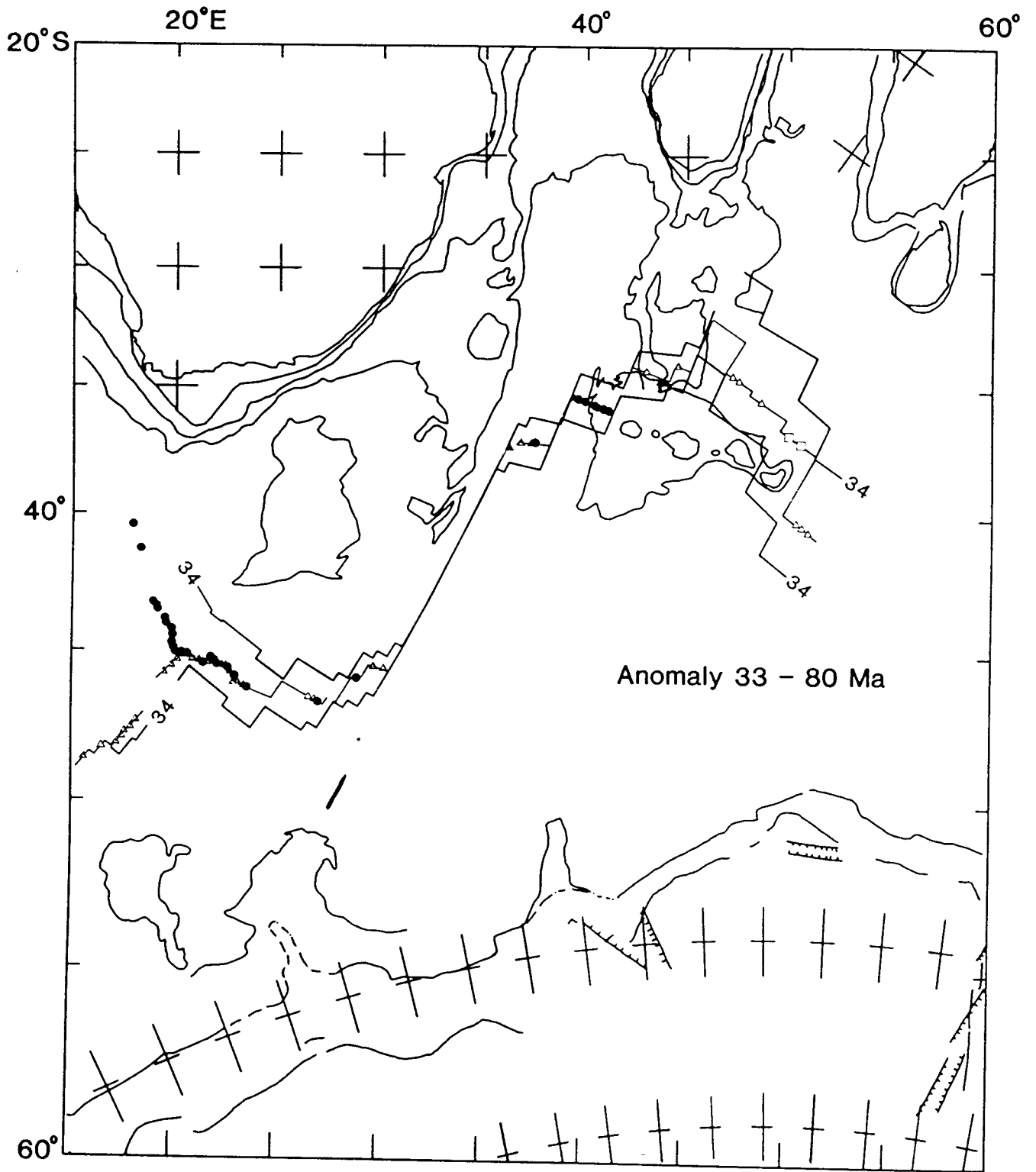


Figure 6b

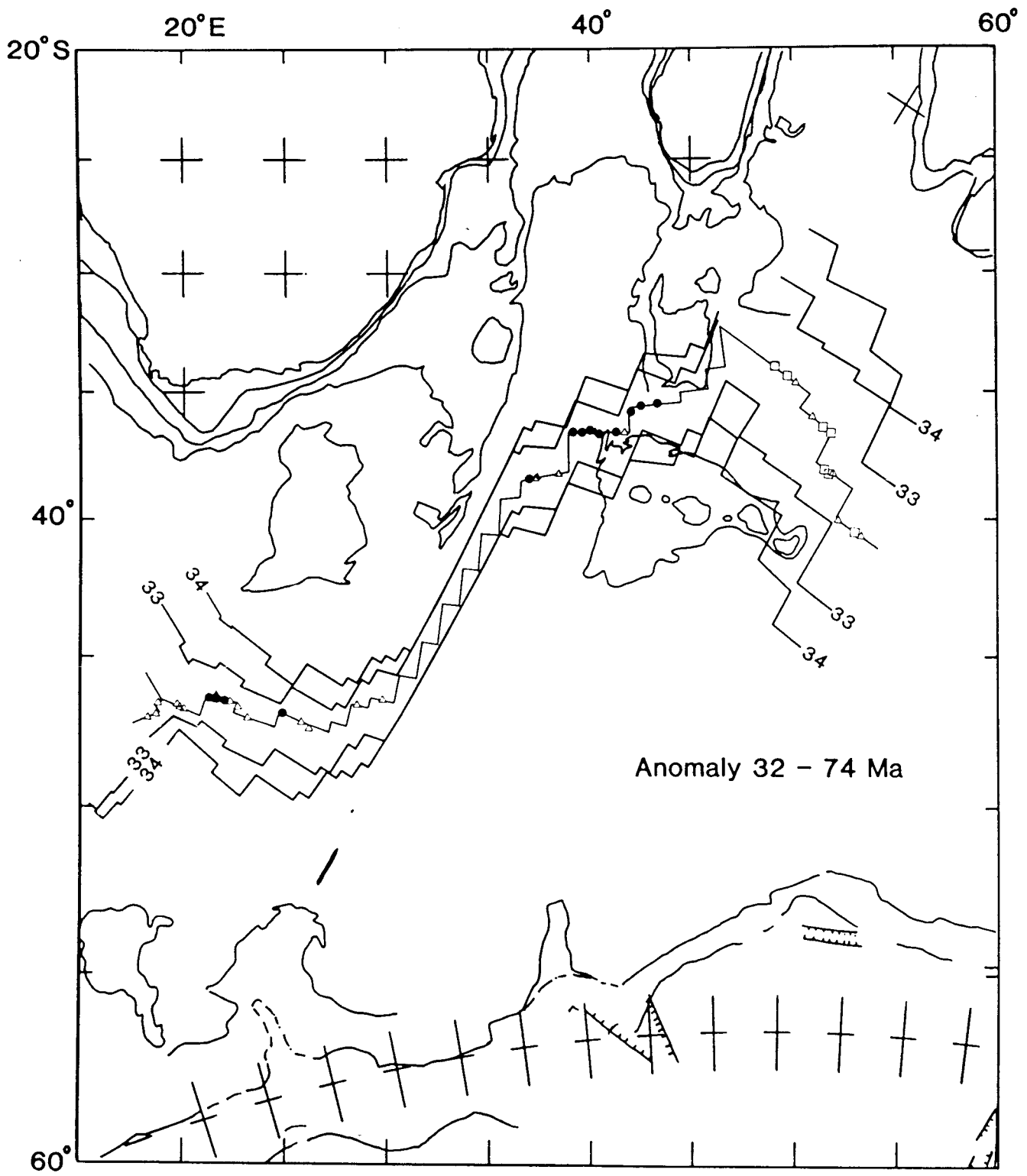


Figure 6c

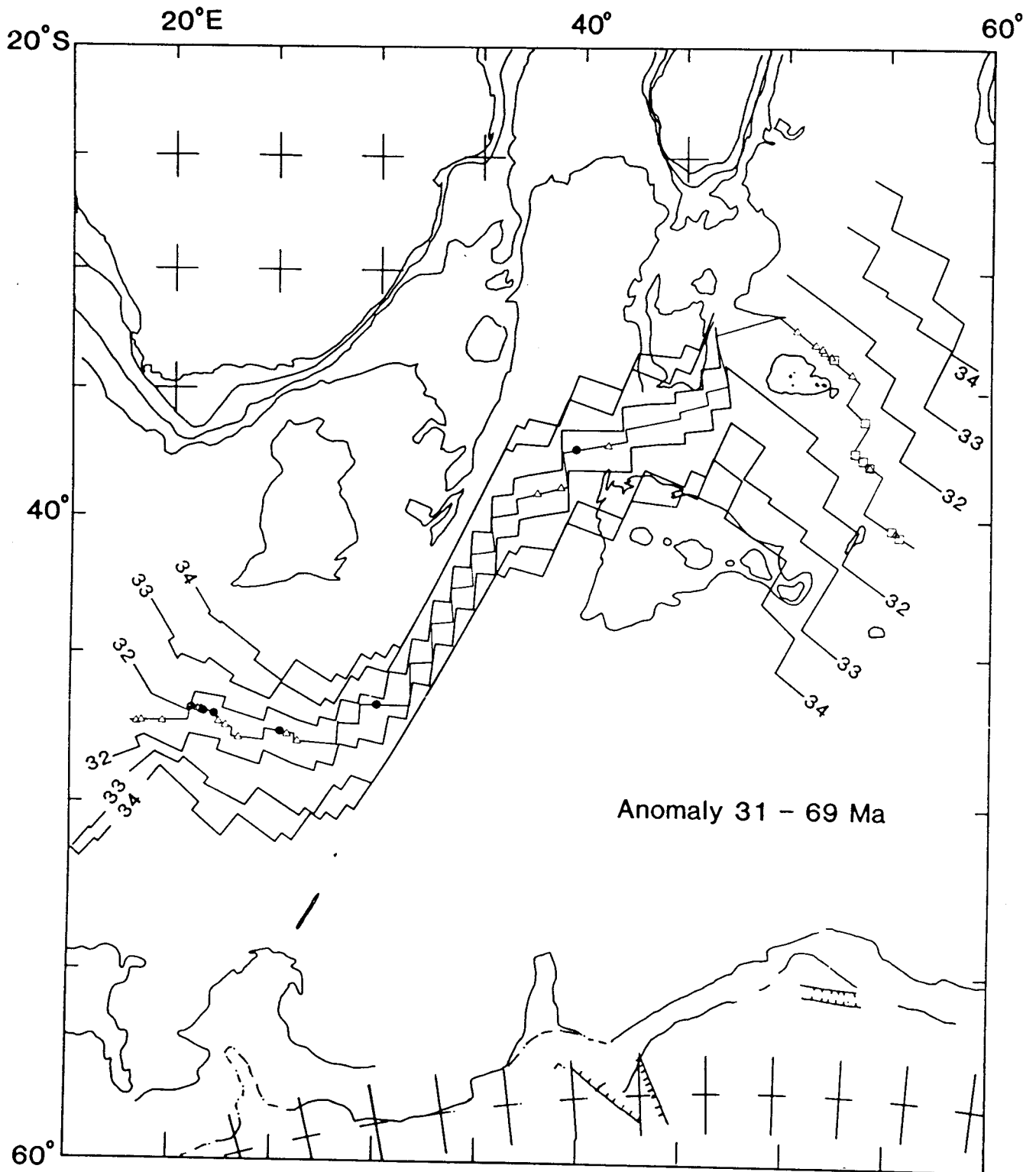


Figure 6d

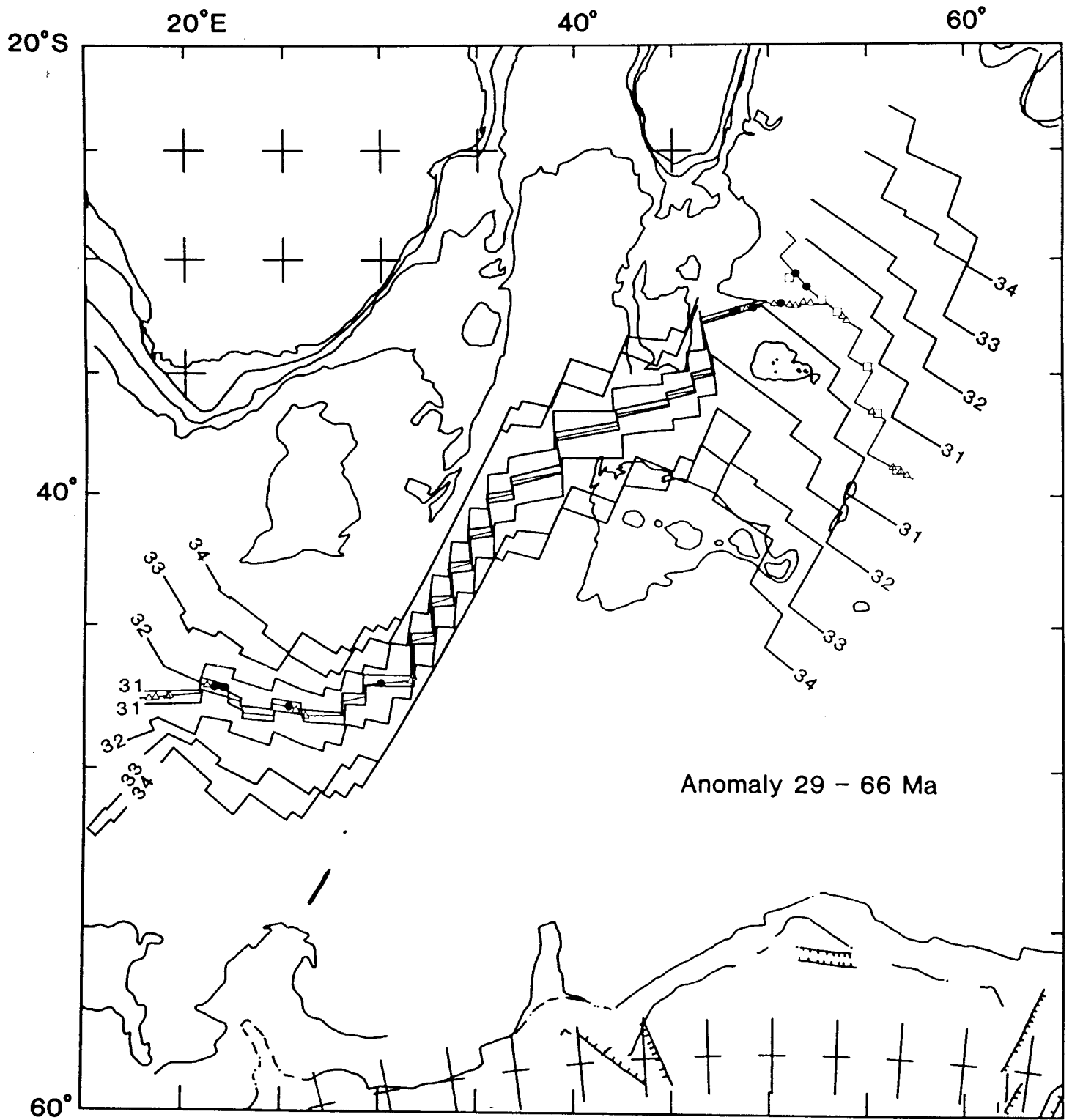


Figure 6e

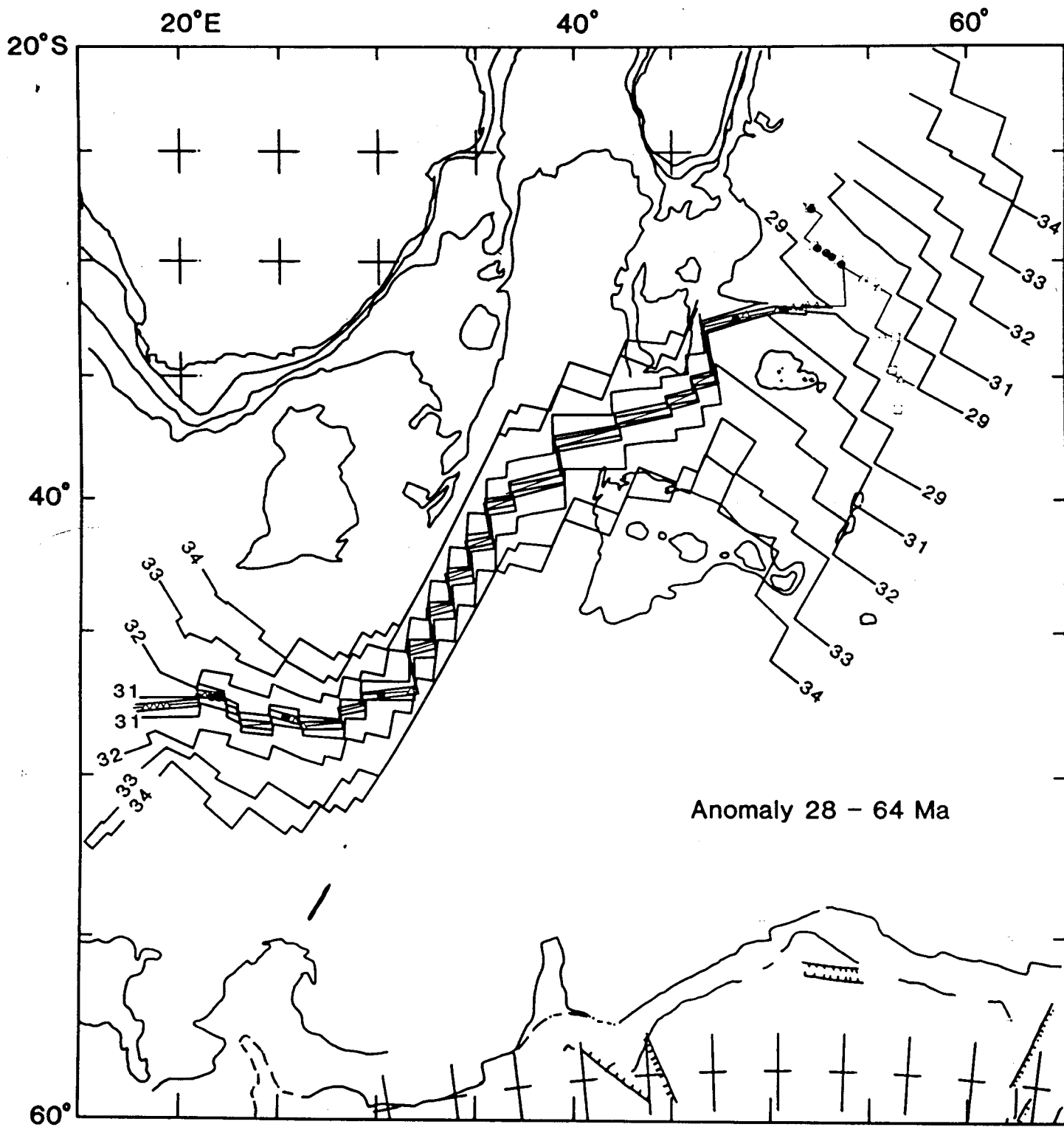


Figure 6f

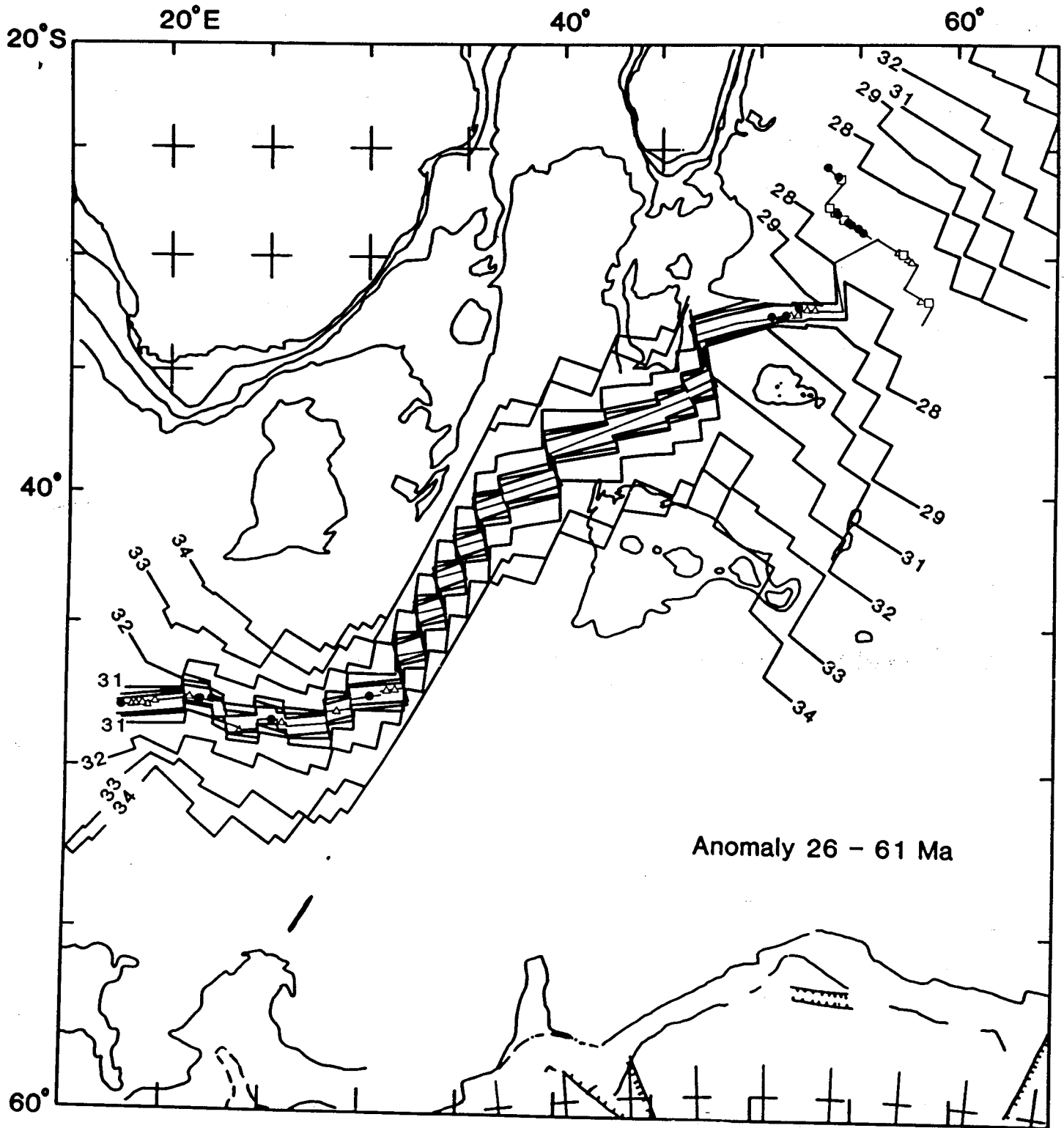


Figure 6g

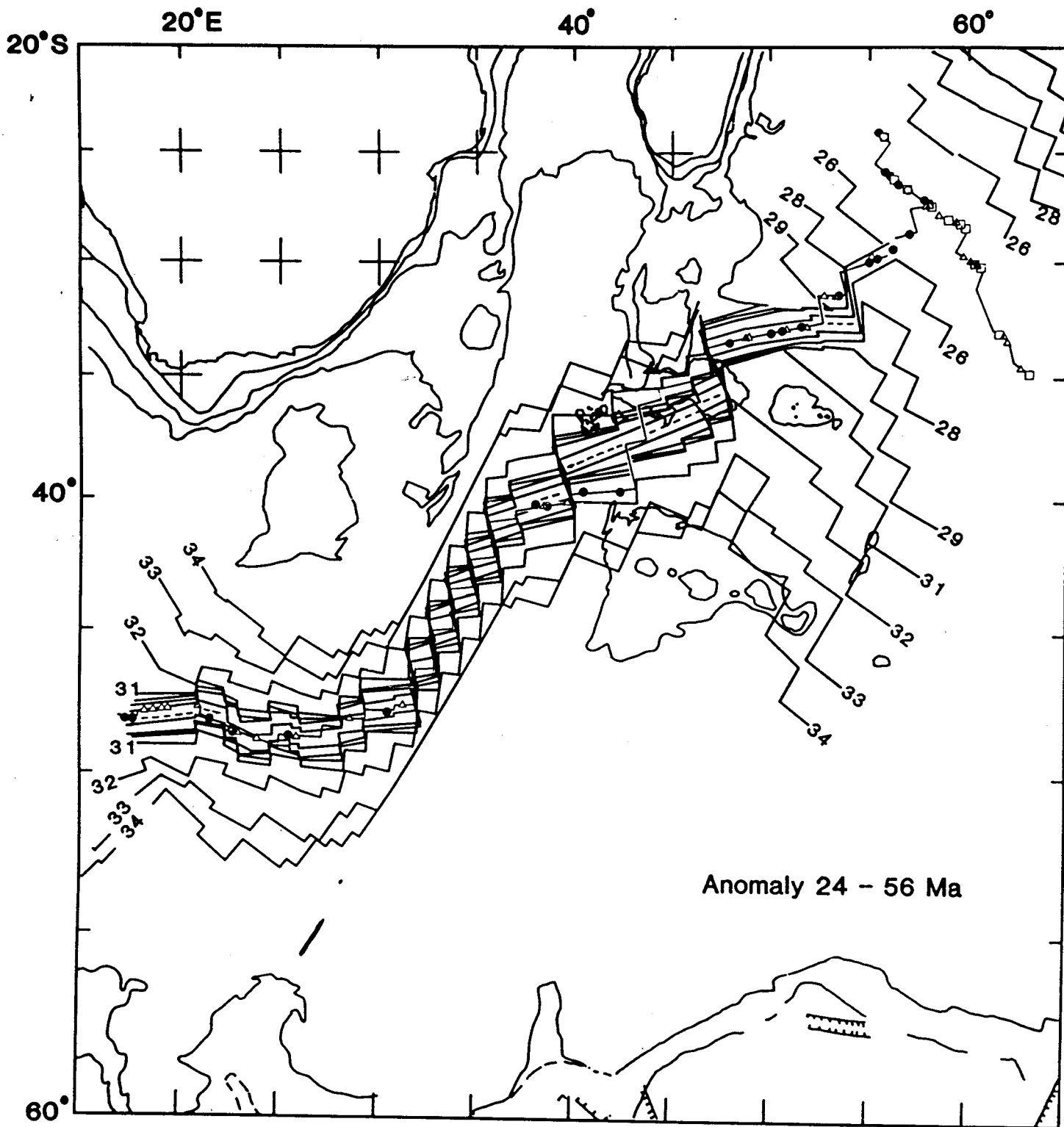


Figure 6h

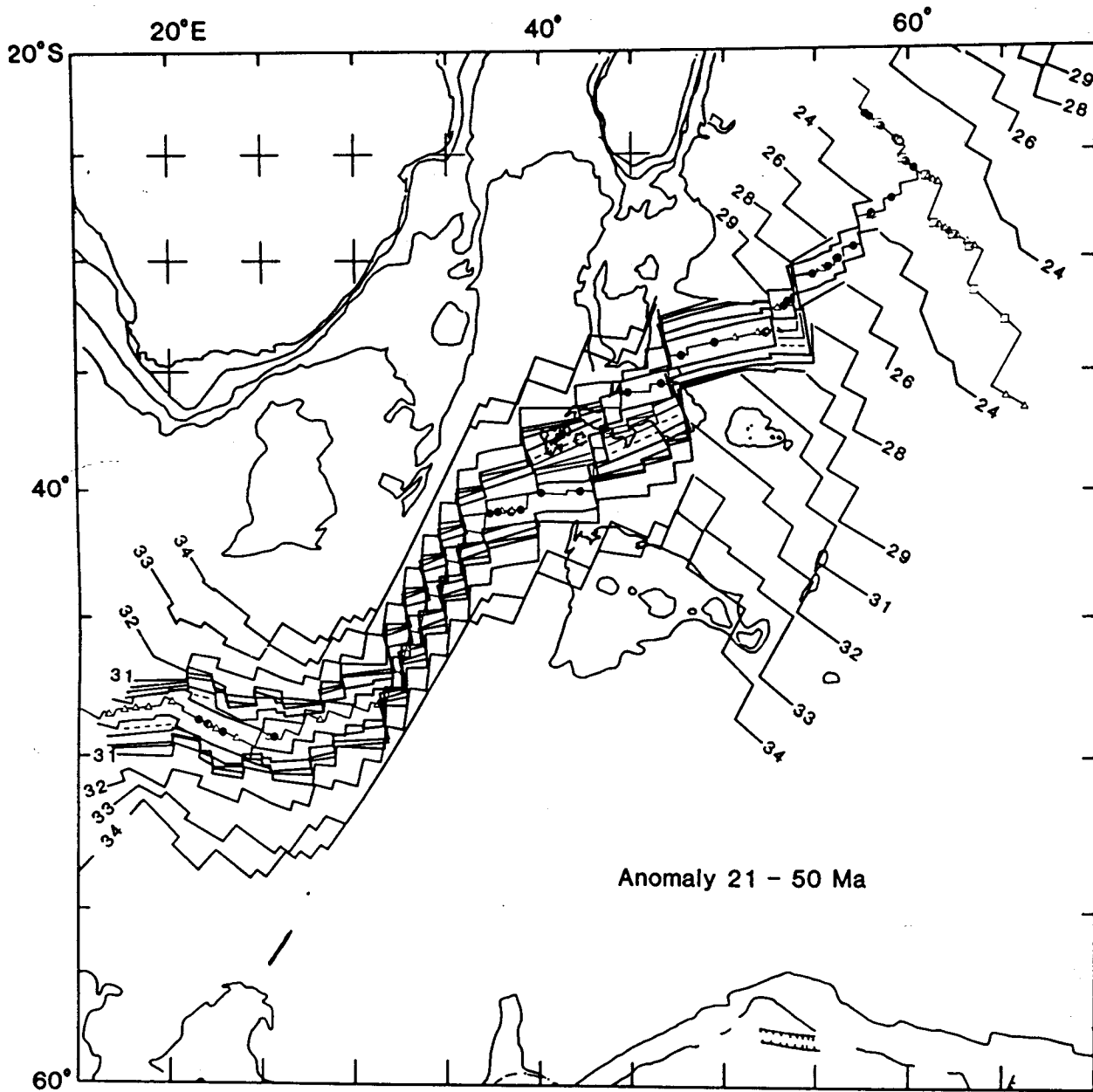


Figure 6i

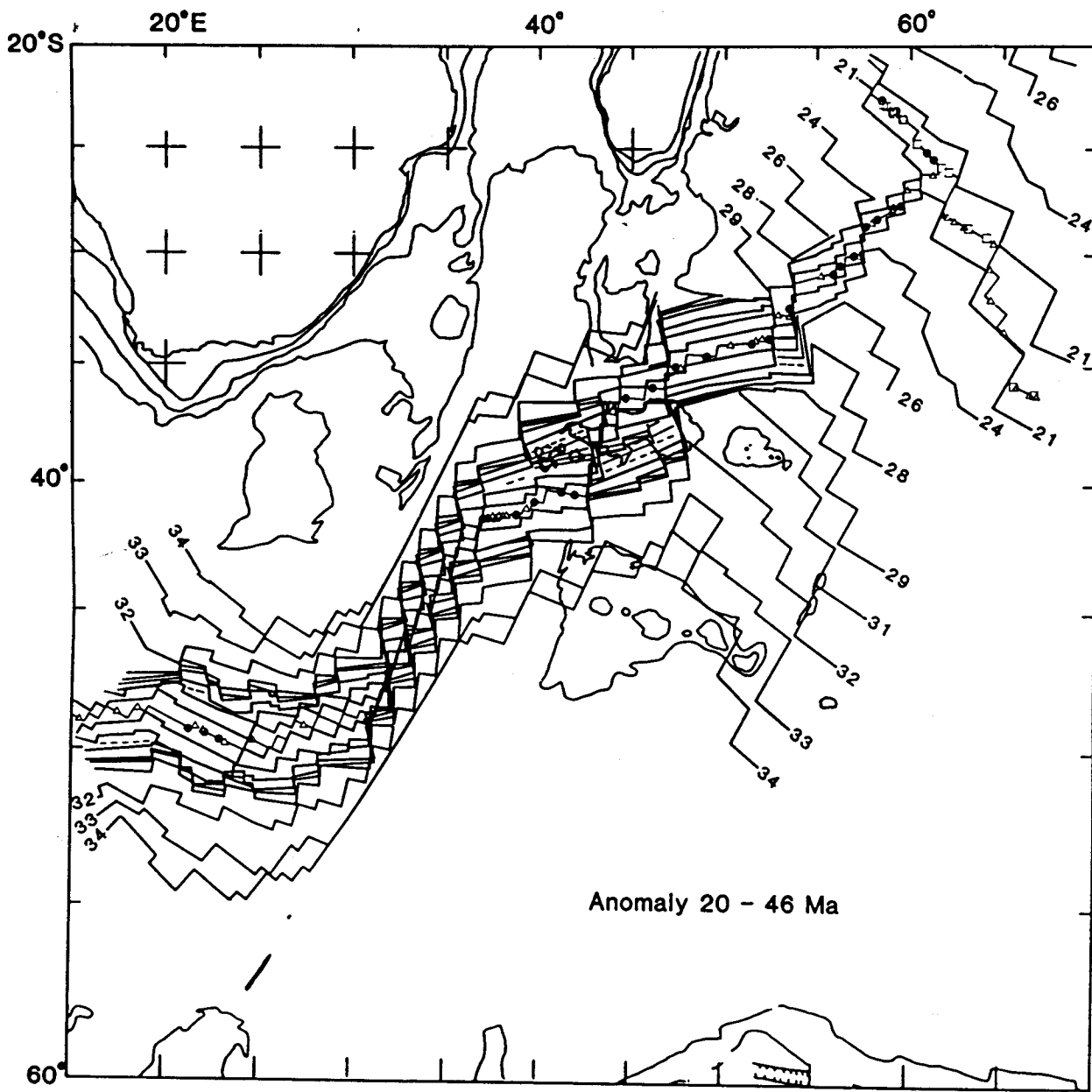


Figure 6j